Continuous cascades in the wavelet space as models for synthetic turbulence

Jean-François Muzy*
SPE UMR 6134, CNRS, Université de Corse, 20250 Corte, France

(Received 7 December 2018; published 10 April 2019)

We introduce a wide family of stochastic processes that are obtained as sums of self-similar localized "wave forms" with multiplicative intensity in the spirit of the Richardson cascade picture of turbulence. We establish the convergence and the minimum regularity of our construction. We show that its continuous wavelet transform is characterized by stochastic self-similarity and multifractal scaling properties. This model constitutes a stationary, "grid free" extension of $\mathcal{W}$ cascades introduced in the past by Arneodo, Bacry, and Muzy using a wavelet orthogonal basis. Moreover, our approach generically provides multifractal random functions that are not invariant by time reversal and therefore is able to account for skewed multifractal models and for the so-called "leverage effect." In that respect, it can be well suited to providing synthetic turbulence models or to reproducing the main observed features of asset price fluctuations in financial markets.

DOI: 10.1103/PhysRevE.99.042113

I. INTRODUCTION

The goal of modeling the observed "random" fluctuations of the velocity field and the intermittent character of the small-scale dissipated energy in fully developed turbulent flows has played a critical role in the development of mathematical concepts around multifractal processes. In particular, random multiplicative cascades first considered by the Russian school [1–3] and subsequently developed by Mandelbrot [4,5] in order to mimic the energy transfer from large to small scales [6] represent the paradigm of multifractal random distributions. They are the basis of much mathematical work and have led to a wide number of applications far beyond the field of turbulence.

Mandelbrot cascades ($\mathcal{M}$ cascades) mainly consist of building a random measure by using a multiplicative iterative rule. One starts with some large interval with a constant measure density W_0 and splits this interval into two equal parts. The measure density in the left and right parts are obtained by multiplying W_0 by respectively two independent, identically distributed positive factors (say W_1^L and W_1^R). This operation is then repeated independently on the two subintervals and so on, *ad infinitum*, in order to converge towards a singular measure whose properties have been studied extensively (see, e.g., [5,7–9]). The main disadvantage of $\mathcal{M}$ cascades is that they involve a specific scale ratio ($s = 2$ in general) and are limited to living in the starting interval. This lack of stationarity and continuous scale invariance is obviously not suited to accounting for natural phenomena. In order to circumvent these problems, continuous extensions of Mandelbrot cascades were proposed by first Barral and Mandelbrot [10] and later by Bacry and Muzy [11,12]. The idea under these constructions is to replace the discrete multiplicative density $\prod_{i=1}^{n} W_i = e^{\sum_{i=1}^{n} \ln W_i}$ with $e^{\omega_\ell(t)}$, where $\omega_\ell(t)$ is an infinitely divisible noise chosen with a logarithmic correlation function designed to mimic the treelike (in general a dyadic tree) structure underlying $\mathcal{M}$ cascades [13–15].

The above definitions of random cascade measures led to a large number of extensions notably in order to construct stochastic processes with some predefined regularity properties. The most popular approach was initiated by Mandelbrot (see, e.g., [16]) and consists of compounding a self-similar stochastic process such as the (fractional) Brownian motion $B_H(t)$ with a "multifractal time" $M(t)$, a multifractal measure of the interval $[0, t]$ as provided by a continuous cascade. Such a compounded process $B_H(M(t))$ inherits the multifractal scaling properties of $M(t)$ with a "main" regularity that corresponds to the self-similar process $B_H(t)$. An alternative but related approach was initially proposed with the construction of "the multifractal random walk" (MRW) in Refs. [14,17] and consists of interpreting $M(dt)$ as the local variance of a fractional Brownian motion $B_H(t)$. As emphasized in Refs. [11,18,19], this amounts to constructing a multifractal process as (the limit of) a stochastic integral such as $\int e^{\omega_\ell(t)} dB_H(t)$. This point of view is inspired by classical stochastic volatility models of financial markets that aim at accounting for the observed bursts in price fluctuations by the random nature of the variance of an underlying Gaussian law. It can also be understood as a formalization of the so-called "Kolmogorov refined similarity hypothesis" [6] according to which the velocity fluctuation δv and the local rate of dissipated energy ε are related as, in its Lagrangian version [20], $\delta_\tau v \sim \varepsilon_\tau^{1/2} dW_\tau$, dW_τ being a noise such that $\mathbb{E}[dW_\tau^2] = \tau$. Accordingly, the multifractal properties of the velocity field directly come from those of the local dissipation field ε, a multifractal cascade interpreted as a "local variance." The main advantage of continuous cascades and their associated random processes is that they provide a large class of parsimonious models with stationary increments and continuous stochastic scale invariance properties. From a practical point of view, they are easy to calibrate from data and can provide simple analytical or numerical solutions to many statistical problems. However, the aforementioned

*muzy@univ-corse.fr

methods to derive a multifractal process from a multifractal measure lack flexibility and in particular hardly allow one to describe processes that are not invariant by time reversal. This means that the increment distribution skewness (i.e., nonvanishing third-order moments of the increments at different scales) as observed in turbulence, or the leverage effect (i.e., some causal, asymmetric relationship between increment signs and increment amplitudes) as observed in financial time series, cannot be captured easily within this framework. All former attempts to address this issue were based on studying a random noise such as $e^{\omega_\ell(t)}\Delta B_H(t)$ for a specific cross-covariance between ω_ℓ and ΔB_H [21,22]. However, as discussed in Ref. [22], this approach leads to a nondegenerated limiting process only in some restricted range $H > 1/2$ and therefore cannot be used as a model for financial markets ($H \simeq 1/2$) or turbulence ($H \simeq 1/3$). More recently, Chevillard *et al.* [23] introduced a new model that obeys multifractal scaling with a (signed) third-order structure function that behaves as a linear function, like in turbulence. This model is defined within the context of Gaussian multiplicative chaos [i.e., a Gaussian version of $\omega_\ell(t)$] and mainly consists of considering a fractional integration of a product such as $\omega' e^{\omega} dB$, where ω' represents a peculiar intermittent version of ω, independent of ω but correlated with the white noise dB. The authors have shown that their construction leads to a properly defined intermittent skewed random process. However, we can point out that the model of Chevillard *et al.* is far from being simple, involves cumbersome computations, and is not characterized by self-similar properties; it follows a multifractal scaling only in the limit of small scales.

In this paper, we propose a different path to solve the challenging issue of mixing multiscaling properties and noninvariance by time reversal. Beyond this question, our construction also offers an appealing alternative way to build a large class of multifractal functions with well-controlled scaling (or regularity) properties and that are characterized by new features as compared to former constructions. Our approach is directly inspired by the random cascade picture originally proposed by Richardson [24] under which, in turbulent flows, large eddies are stretched and broken into smaller ones to which they transfer a fraction of their energy and so on, up to the dissipation scale. Instead of trying to capture the velocity field intermittency from the final state of such a cascade, i.e., the dissipation field (which is a multifractal measure), the previous scenario suggests that one could describe the overall flow as a *superposition* of coexisting structures at all scales correlated with each other by a cascading intensity (energy). This viewpoint of decomposing a function as a weighted sum of wave forms (the "eddies") at different scales precisely corresponds to a wavelet transform representation [25]. The construction of discrete multiplicative cascades along the wavelet tree associated with the orthogonal wavelet basis was already proposed two decades ago by Arneodo, Bacry, and Muzy [26]. These "$\mathcal{W}$ cascades" have proven to be an appealing alternative to $\mathcal{M}$-cascade-based constructions in order to directly build multifractal stochastic processes [13,27]. They also provided a suitable approach to extend the framework of stochastic self-similarity and build new random functions with a nontrivial spectrum of oscillating singularities [28,29]. Our goal in this paper is thus to construct an extension of $\mathcal{W}$ cascades in order to get rid of the restraining grid structure of the wavelet orthogonal basis that prevents, very much like grid-bounded $\mathcal{M}$ cascades, $\mathcal{W}$ cascades from being able to simply account for stationarity and continuous scale invariance. For that purpose, we simply consider a continuous sum over space t and scales ℓ of "synthesizing wavelets" weighted by a factor that is precisely given by the stochastic density involved in continuous cascades, $e^{\omega_\ell(t)}$. We show that such a construction allows us to obtain well-defined processes with a large flexibility on their scaling and regularity properties. Moreover it generically leads to skewed processes and is able to reproduce the leverage effect for specific shapes of synthesizing wavelets. In that respect, they can naturally be invoked as models for synthetic turbulence or calibrated to account for asset fluctuations in financial markets. Various numerical examples are provided throughout the paper in order to illustrate our purpose and notably to show the model's ability to reproduce many of the observed features of the longitudinal velocity field fully developed by turbulence experiments.

The paper is structured as follows: In Sec. II we recall the main lines of continuous-cascade (Sec. II A) and $\mathcal{W}$-cascade (Sec. II B) constructions. This notably allows us to introduce the process $\omega_\ell(t)$ and review its main statistical properties. Our construction of continuous cascades in the wavelet plane ($\mathcal{CW}$ cascades) is introduced in Sec. III. After the definition and the statement of a weak convergence result, we provide some numerical examples (Sec. III A). In Sec. III B, we study their wavelet transform and establish the almost sure minimum regularity of their paths. Scaling and self-similarity properties of this class of processes are studied in Sec. IV. We prove that their structure functions are characterized by a power-law behavior with some nonlinear ζ_q spectrum of scaling exponents (Sec. IV A) and study the correlation functions of the absolute increments (Sec. IV B). We finally study the properties of $\mathcal{CW}$ cascades with respect to time reversal, notably the behavior of the skewness and the leverage function (Sec. V). Concluding remarks and prospects for future research are given in Sec. VI while technical material and proofs are provided in appendices.

II. CONTINUOUS CASCADES AND $\mathcal{W}$ CASCADES

This section contains a brief review of the notions of "continuous" and "wavelet" multiplicative cascades. The first ones were introduced as stationary, self-similar singular measures with log-infinitely divisible multifractal properties while $\mathcal{W}$ cascades are the wavelet transform counterparts of Mandelbrot discrete multiplicative cascades. As explained in Sec. III, both constructions will be mixed in order to build continuous wavelet cascade models.

A. Log-infinitely divisible continuous cascades

Continuous random cascades are stochastic measures $M(t)$ introduced few years ago [10–12,17,30] in order to extend, within a stationary and grid-free framework, the Mandelbrot discrete multiplicative cascades. Such a measure $M(t) = \int_0^t dM_u$ can have exact multifractal scaling properties in the

sense that it satisfies, for a given $T > 0$, $\forall t \leqslant T$,

$$\mathbb{E}[M(t)^q] = K_q \left(\frac{t}{T}\right)^{\zeta_q}, \tag{1}$$

where ζ_q is a nonlinear concave function called the multifractal spectrum (or the spectrum of structure functions scaling exponents in the context of turbulence [6,31]) and K_q is an (eventually infinite) prefactor corresponding the the q-order moment at scale $t = T$.

In Refs. [11,12] (see also [10]) $dM(t)$ is obtained as the (weak) limit, when $\ell \to 0$ of the measure with density,

$$dM_\ell(t) = e^{\omega_\ell(t)} dt, \tag{2}$$

where $e^{\omega_\ell(t)}$ is a stationary log-infinitely divisible process representing the continuous cascade from scale T to scale ℓ. Its precise definition and main properties, reviewed in Appendix A, notably imply that it satisfies [thanks to Eqs. (A4) and (A5)]

$$\mathbb{E}[e^{q\omega_\ell(t)}] = \left(\frac{T}{\ell}\right)^{\phi(q)}, \tag{3}$$

where $\phi(q)$ is the cumulant generating function associated with an infinitely divisible law as provided by the celebrated Levy-Khintchine theorem [32]. Moreover, $\omega_\ell(t)$ verifies, $\forall s < 1$, $u \in [0, T]$,

$$\omega_{s\ell}(su) \overset{\mathcal{L}}{=} \Omega_s + \omega_\ell(u), \tag{4}$$

where $\overset{\mathcal{L}}{=}$ means that the two processes have the same finite-dimensional distributions of any order and Ω_s is a random variable independent of the process $\omega_\ell(t)$ with the same distribution as $\omega_{sT}(t)$. The multifractal scaling (1) follows since Eq. (4) entails

$$\begin{aligned} M(st_0) &= \lim_{\ell\to 0} \int_0^{st_0} e^{\omega_{s\ell}(u)} du \overset{\mathcal{L}}{=} s e^{\Omega_s} \lim_{\ell\to 0} \int_0^{t_0} e^{\omega_\ell(u)} du \\ &= s e^{\Omega_s} M(t_0), \end{aligned} \tag{5}$$

and thus by choosing $t_0 = T$ and $s = t/T$, we have

$$\mathbb{E}[M(t)^q] = s^q \mathbb{E}[e^{q\Omega_s}] \mathbb{E}[M(T)^q]$$

that leads, using Eq. (3), to Eq. (1) with

$$\zeta_q = q - \phi(q).$$

As discussed in the introduction, a large class of multifractal processes $X(t)$ with stationary increments can be obtained from a multifractal measure $M(t)$. One can, as suggested by Mandelbrot [16,33], compound a self-similar process $B_H(t)$ (e.g., a fractional Brownian motion) by the nondecreasing function $M(t)$ so that

$$X(t) = B_H(M(t)).$$

Within this approach $M(t)$ is referred to as the "multifractal time." Since $B_H(st) \overset{\mathcal{L}}{=} s^H B_H(t)$, one has

$$X(st) \overset{\mathcal{L}}{=} s^H e^{H\Omega_s} X(t)$$

that entails, given the increment stationarity of $X(t)$, the multiscaling of the structure functions:

$$\mathbb{E}[|X(t+\tau) - X(t)|^q] = C_q \tau^{\zeta_q}$$

with $\zeta_q = qH - \phi(qH)$. Another approach initiated in Refs. [14,17] (see also [11]) is to consider the limit $\ell \to 0$ of the sequence $X_\ell(t) = \sum_{k=1}^{t/\ell} \ell^\alpha e^{\omega_\ell(k)} dW_k$, where dW_k is a fractional Gaussian noise and α an appropriate constant chosen to ensure the convergence (in some specific sense) of the series. This amounts to interpreting $e^{\omega_\ell(k)}$ as a stochastic variance or, in the field of mathematical finance, a "stochastic volatility." Related constructions consist of considering stochastic integrals such as $\int e^{\omega_\ell(t)} dB_H(t)$, where $B_H(t)$ is a fractional Brownian motion [11,18,19]. All these approaches were extensively used and studied in the literature as paradigms of multifractal processes satisfying exact stochastic scale invariance properties and also considered as toy models for applications such as turbulence or financial time series. However, as recalled in the introduction, they mainly involve separately the construction of a multifractal measure and a self-similar process and do not consist of directly building the random process $X(t)$ with some specific properties. Then there results a lack of flexibility in the obtained features; in particular, as emphasized previously and discussed in Refs. [21–23], skewed statistics and "leverage effect" cannot be obtained in a fully satisfactory way through these approaches. As reviewed below, wavelet cascades offer an interesting alternative in the sense that they do not rely on any preset self-similar process and consist of directly building $X(t)$ with a control of its scaling or regularity properties.

B. $\mathcal{W}$ cascades

In Ref. [26], the authors introduced the so-called $\mathcal{W}$ cascades as the natural transposition of Mandelbrot $\mathcal{M}$ cascades within the framework of an orthogonal wavelet transform. This allows one to construct multifractal processes or distributions with a precise control of their regularity properties. The idea is to build a new class of (multi)fractal functions $Z(t)$ from their explicit representation over a wavelet basis:

$$Z(t) = \sum_{j=0}^{\infty} \sum_{k=0}^{2^{j-1}} c_{j,k} \psi_{j,k}(t), \tag{6}$$

where $\psi_{j,k}(t) = 2^j \psi(2^j t - k)$ and $\{\psi_{j,k}(t)\}_{j,k\in\mathbb{Z}}$ constitutes an orthogonal wavelet basis of the interval. The wavelet coefficients $c_{j,k} = \int Z(u)\psi_{j,k}(u) du$ are chosen according to the multiplicative cascade rule [26]:

$$c_{j,2k} = W_0 c_{j-1,k}, \quad c_{j,2k+1} = W_1 c_{j-1,k}, \tag{7}$$

where W_0 and W_1 are i.i.d. copies of a real-valued random variable W. We see that if W is a positive random variable, the law of the wavelet coefficient $c_{j,k}$ is precisely given by the law of the density of an $\mathcal{M}$ cascade at construction step j:

$$c_{j,k} = \prod_{m=0}^{j} W_m. \tag{8}$$

It has been shown in Ref. [26] that, under some mild condition on the law of W, $Z(t)$ is a well-defined multifractal process with almost surely Lipschitz regular paths. Such a construction of multifractal functions associated with specific random wavelet series has been extended recently by Barral and Seuret [27]. If M stands for a Mandelbrot multifractal

measure (an $\mathcal{M}$ cascade) constructed from an iterative random multiplicative rule as described in the introduction, these authors considered a wavelet random series such as (6) but where $c_{j,k}$ is given by the measure of the associated dyadic interval $I_{j,k} = [k2^{-j}, (k+1)2^{-j}]$:

$$c_{j,k} = 2^{-j\alpha} M(I_{j,k}).$$

Barral and Seuret proved that the scaling and regularity properties of $Z(t)$ are directly inherited from those of $M(t)$. Moreover, they have shown that, under specific conditions, replacing $\prod_{i=1}^{j} W_i$ of $\mathcal{W}$ cascades with the limit measure of the associated dyadic interval, $M(I_{j,k})$, does not change the multifractal properties (see Sec. IV A for more details).

Unlike the constructions of multifractal processes based on multifractal measures, $\mathcal{W}$ cascades allow one to directly build multifractal processes without the need for any additional self-similar process. However, very much like $\mathcal{M}$ cascades, they do involve a dyadic tree and a finite time interval that can hardly be used to fit most of experimental situations. For that reason, in the same manner in which $\mathcal{M}$ cascades have been extended to log-infinitely divisible continuous cascades, we aim at defining a continuous version of $\mathcal{W}$ cascades.

III. CONTINUOUS $\mathcal{W}$ CASCADES

In this section, we introduce the class of models we consider in the paper. Our goal is to extend the previously described $\mathcal{W}$ cascades to a grid-free background. The main idea is to replace the discrete sum (6) by a continuous sum over space and scales and the discrete product in Eq. (8) at scale $\ell = 2^{-j}$ with its "continuous" (i.e., stationary and "grid free") counterpart $e^{\omega_\ell(t)}$ described in Sec. II A and Appendix A.

A. Definition and numerical illustrations

1. Definition and convergence

Let us define a stochastic process $X(t)$ as a (continuous) sum of localized wave forms (i.e., "wavelets") of size ℓ and whose intensity is given by the class of stationary, log-infinitely divisible process $e^{\omega_\ell(t)}$ used in the definition of continuous cascades of Sec. II A.

Let $H > 0, \ell > 0$ and consider the following (well defined) integral:

$$X_\ell(t) = \int_\ell^T s^{H-2} ds \int_{-\infty}^{+\infty} e^{\omega_s(b)} \varphi\left(\frac{t-b}{s}\right) db, \qquad (9)$$

where $\omega_s(u)$ is the infinitely divisible process defined in Sec. II A and $\varphi(t)$ is a wavelet that can be chosen as a square integrable smooth function with compact support (e.g., the interval $[-\frac{1}{2}, \frac{1}{2}]$) and that is sufficiently oscillating so that its first N moments vanish. Hereafter, we will referred to this wavelet as the "synthesizing wavelet." As emphasized below, this amounts, in some sense, to interpreting $s^H e^{\omega_\ell(t)}$ as the continuous wavelet transform of $X(t)$ at time t and scale ℓ, Eq. (9) corresponding to the continuous wavelet reconstruction formula. Let us remark that if $\phi(1) < \infty$, one can, without loss of generality (since it simply consists of redefining the parameter H), always assume that in Eq. (9), $\omega_s(t)$ is chosen such that

$$\mathbb{E}[e^{\omega_s(t)}] = 1 \Leftrightarrow \phi(1) = 0. \qquad (10)$$

In Appendix B, we establish the weak convergence of $X_\ell(t)$ in the space of continuous functions when $\ell \to 0$. Namely, we show that the weak limit

$$\lim_{\ell \to 0} X_\ell(t) = X(t) \qquad (11)$$

exists as a continuous function provided

$$H > \frac{\phi(2)}{2}. \qquad (12)$$

We will call such a limit $X(t)$ a "continuous wavelet cascade" process or a $\mathcal{CW}$ cascade. Let us notice that condition (12) is precisely the analog of the condition for L^2 convergence of $\mathcal{W}$ cascades established by Arneodo *et al.* (condition $H1$ of Proposition 1 in Ref. [26]).

2. Numerical examples

In numerical experiments, one has to choose the infinitely divisible law of the process $\omega_\ell(t)$, the regularity parameter H, the integral scale T, and the synthesizing wavelet $\varphi(t)$. The simulation procedure simply consists of a discretization of Eq. (9). Its main lines are described in Appendix D.

Despite that our approach allows us to construct $\mathcal{CW}$ cascades associated with any bona fide log-infinitely divisible statistics, all the examples provided in the paper involve log-normal cascades, which are the simplest ones to handle and which involve a single variance parameter λ^2. As far as turbulence is concerned, the log-normal hypothesis can be questionable and we could also have considered, e.g., a She-Lévêque log-Poisson model [34] that is very popular to account for observed scaling properties. However, experimental data hardly allow one to distinguish log-normal and log-Poisson models because of the so-called "linearization effect" for high values of the order increment structure functions [35]

In the log-normal case, $\omega_\ell(t)$ is a Gaussian process with a covariance function given by expression (A4). In that respect, thanks to condition (10), the function $\phi(q)$ simply reads

$$\phi(q) = \frac{\lambda^2}{2} q(q-1), \qquad (13)$$

and the condition (12) becomes $\lambda^2 < 2H$. Let us remark that this condition appears to be less restrictive than the condition of existence of a MRW $\lambda^2 < 1/2$ [17,36] and it is *a priori* possible to build $\mathcal{CW}$ cascades with a large intermittency coefficient.

Among the choices we made for the synthesizing wavelets φ there is the class of smooth variants of the Haar wavelet:

$$h^{(n)}(t) = \left(\underbrace{\mathbb{I} \star \ldots \star \mathbb{I}}_{n} \star h\right)(t), \qquad (14)$$

where $\mathbb{I}(t)$ is the indicator function of the interval $[0, 1/2)$, $h(t) = \mathbb{I}(t+1/2) - \mathbb{I}(t)$ is the Haar wavelet, and $\star$ stands for the convolution product. Notice that $h^{(n)}(t)$ has one vanishing moment and is of class $C^{n-1}(\mathbb{R})$. We also use wavelets in the class of the derivatives of the Gaussian function:

$$g^{(n)}(t) = \frac{d^n}{dt^n} e^{-\frac{x^2}{2}}. \qquad (15)$$

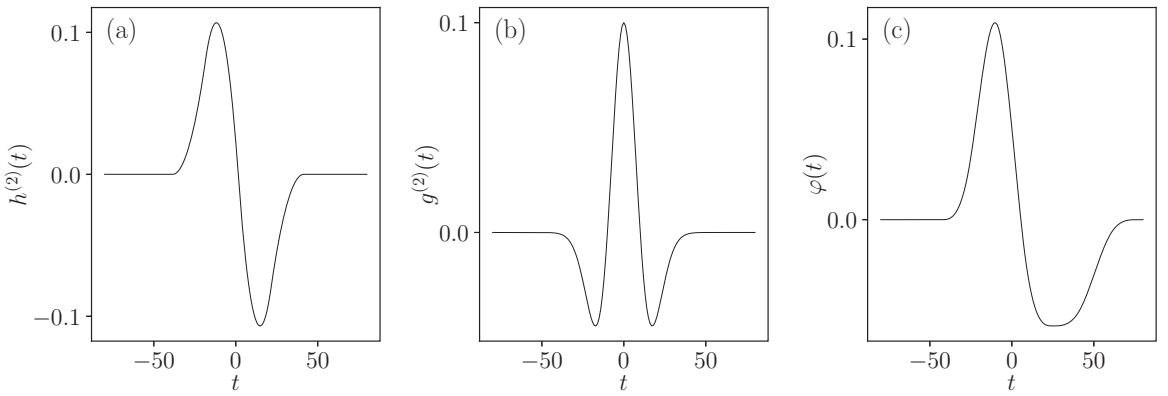

FIG. 1. Examples of synthesizing wavelets $\varphi(t)$. (a) The compactly supported odd function $h^{(2)}(t)$ [Eq. (14)]. (b) The "Mexican hat," i.e., the even wavelet $g^{(2)}(t)$ [Eq. (15)]. (c) A nonsymmetric wavelet obtained by smoothing an asymmetric version of the Haar wavelet.

Some examples among these wavelet classes are plotted in Fig. 1 (dilation and normalization factors are arbitrary). Note that one can also consider asymmetric wavelets such as the one illustrated in the right panel of Fig. 1 that is constructed by asymmetrizing and smoothing the Haar wavelet (see Sec. V for a usage of asymmetric wavelets).

Some examples of sample paths of $X(t)$ are plotted in Fig. 2. All processes were generated using a Gaussian process $\omega_\ell(t)$ with the intermittency coefficient $\lambda^2 = 0.025$ and the integral scale $T = 2048$. The synthesizing function was chosen to be $\varphi(t) = h^{(3)}(t)$. The scaling parameter H has been chosen to be respectively $H = 0.36$, $H = 0.51$, and $H = 0.76$ from top to bottom. One can see that H directly controls the global regularity of the paths: the larger H, the more regular the path of $X(t)$ is. This is the analog of the parameter H of the fractional Brownian motion [37]. It is noteworthy that despite that $X(t)$ appears to be a process with zero mean stationary increments, unlike all constructions proposed so far for multifractal stationary processes, it does not involve any supplementary "white" or "colored" noise, like the Gaussian white noise, since it is only based on the "intensity" process $e^{\omega_\ell(t)}$ as a source of randomness (see the remark at the end of the next section).

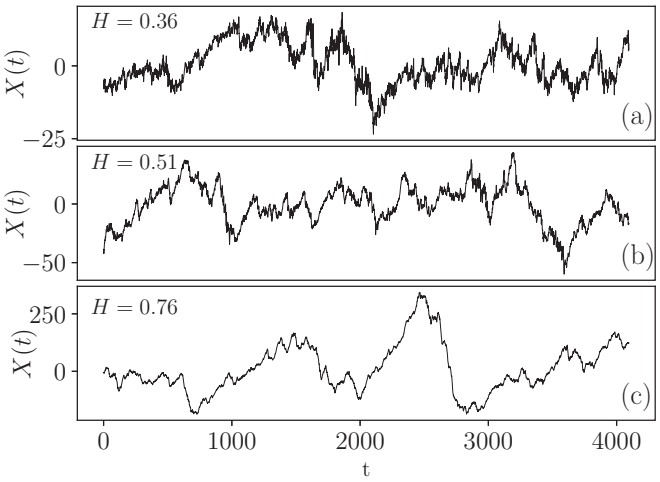

FIG. 2. Sample paths of continuous log-normal $\mathcal{W}$ cascades $X(t)$ corresponding to 3 different values of the parameter H: (a) $H = 0.36$, (b) $H = 0.51$, and (c) $H = 0.72$. In all cases, the intermittency coefficient and the integral scale were chosen to be respectively $\lambda^2 = 0.025$ and $T = 1024$, and the synthesizing wavelet the C^2 version of the Haar wavelet, $h^{(3)}(t)$.

B. Wavelet transform, global regularity, and reconstruction formula

In order to study and characterize the limiting process $X(t)$, one can compute its wavelet transform [25]. If $\psi(t)$ stands for some analyzing wavelet, let us introduce the kernel $K_{\varphi,\psi}(x, s)$ defined as

$$K_{\varphi,\psi}(x, s) = s^{-1} \int \varphi(t)\psi\left(\frac{t-x}{s}\right)dt. \tag{16}$$

The wavelet transform of $X(t)$ can then be simply expressed as

$$\begin{aligned} W(x, a) &= a^{-1} \int X(t)\psi\left(\frac{t-x}{a}\right)dt \\ &= \int_0^T s^{H-2}ds \int_{-\infty}^{+\infty} db\, e^{\omega_s(b)} K_{\varphi,\psi}\left(\frac{x-b}{s}, \frac{a}{s}\right). \end{aligned} \tag{17}$$

It is easy to show that if ψ has more than N vanishing moments one has $K_{\varphi,\psi}(x, s) \sim s^N$ when $s \ll 1$ while if φ has also at least N vanishing moments, then $K_{\varphi,\psi}(x, s) \sim s^{-(N+1)}$ when $s \gg 1$. In that respect, for each x, $K_{\varphi,\psi}(x, s)$ is maximum around $s = 1$. Moreover, if ψ is also supported by $[-1/2, 1/2]$, then $K(x, s) = 0$ if $|x| \geqslant s$. In the sequel, for the sake of simplicity and to avoid cumbersome considerations about the tails of $K(x, s)$ for large and small s, we will suppose that the kernel $K(x, s)$ is nonvanishing only in the time scale interval $s \in [\kappa s, 1]$, $x \in [-s, s]$ for some $\kappa < 1$. Under this assumption, the wavelet transform of $X(t)$ can be

approximated as

$$W(x,a) \simeq \begin{cases} \int_{\kappa a}^{\min(T,a)} s^{H-2} ds \int_{x-a}^{x+a} e^{\omega_s(b)} K_{\varphi,\psi}\left(\frac{x-b}{s}, \frac{a}{s}\right) db, & \text{if } \kappa a \leqslant T, \\ 0, & \text{otherwise.} \end{cases} \tag{18}$$

Let us remark that in the case in which one chooses the analyzing wavelet $\psi(t) = \delta^{(1)}(t)$ with

$$\delta^{(1)}(t) = \delta(t+1) - \delta(t), \tag{19}$$

where $\delta(t)dt$ stands for the Dirac distribution, then $W(t,a)$ is nothing but the increment of $X(t)$ at scale a [38]:

$$W(t,a) = \delta_a X(t) = X(t+a) - X(t). \tag{20}$$

Despite that this "poor man's wavelet" does not possess the requested regularity and oscillating properties [in particular approximation (18) is not supposed to hold], in the sequel, we will often consider that the increment statistics can be deduced from the wavelet transform statistics as a particular case (see, e.g., [38] for a discussion on this specific topic). Along the same line, if $\psi(t) = \delta^{(2)}(t)$, with

$$\delta^{(2)}(t) = \delta(t+2) + \delta(t) - 2\delta(t+1), \tag{21}$$

then $W(t,a)$ corresponds to the increments of second order of $X(t)$: $W(t,a) = X(t+2a) + X(t) - 2X(t+a)$. Hereafter, we will refer to increments of first or second order when it is necessary to distinguish these two specific types of wavelet transforms.

Let us define the spectrum of structure function scaling exponents

$$\zeta_q = qH - \phi(q) \tag{22}$$

and consider its Legendre transform:

$$F(h) = 1 + \inf_q (qh - \zeta_q). \tag{23}$$

Let us suppose that $\exists \eta > 0$ such that $F(h) < 0$ for all $0 \leqslant z < \eta$. In Appendix B, we use expression (18) to show that, for any $L > 0$, almost surely, the paths of $X(t)$ have a uniform Lipschitz regularity α on $[0, L]$ for all $0 < \alpha < h_{\min}$ with

$$h_{\min} = \arg\max\{F(h) < 0\}_{h < H - \phi'(0)}.$$

This result about the almost sure regularity of the paths $X(t)$ extends to continuous $\mathcal{W}$ cascades a property similar to that proven by Arneodo *et al.* in the case of discrete $\mathcal{W}$ cascades [26]. For example, in the log-normal case, $\phi(q)$ is provided in Eq. (13) and therefore $h_0 = H - \phi'(0) = H + \frac{\lambda^2}{2}$. Since $F(h) = 1 - \frac{(h-h_0)^2}{2\lambda^2}$, we obtain, provided $H > \sqrt{2\lambda^2} - \frac{\lambda^2}{2}$, $h_{\min} = h_0 - \sqrt{2\lambda^2} > 0$.

Let us notice that, unlike discrete $\mathcal{W}$ cascades, the weighting process $s^H e^{\omega_\ell(t)}$ involved in the continuous version is always positive. Nevertheless, let us remark that wavelet analysis is also helpful to show that, in the construction (9), instead of choosing the (positive) weights $s^H e^{\omega_s(b)}$, one could equivalently build $X(t)$ from a zero mean weighting process that has the same law as $W(b,s)$, the wavelet transform of $X(t)$. Indeed, let us consider the following process:

$$X'(t) = \lim_{\ell \to 0} \lim_{R \to \infty} \int_\ell^R ds\, s^{-2} \int_{-\infty}^{+\infty} W(b,s) \varphi\left(\frac{t-b}{s}\right) db, \tag{24}$$

where $W(b,s)$ is the wavelet transform of $X(t)$ as defined in Eq. (17). According to the wavelet pointwise reconstruction formula (e.g., as introduced in Ref. [39]), if the analyzing wavelet ψ satisfies some mild conditions with respect to the synthesizing wavelet φ, one expects that $X'(t) = X(t)$ at every point of continuity of $X(t)$. It thus results that (24) provides a whole family of versions of continuous $\mathcal{W}$-cascade construction where the weights are chosen to be a zero mean process as simply obtained from any wavelet transform of the original $X(t)$ function.

IV. SELF-SIMILARITY AND SCALING PROPERTIES

In this section we study the scaling and self-similarity properties of $X(t)$ as defined in Eqs. (9) and (11).

A. Stochastic self-similarity of the wavelet transform and multifractal scaling

Let us first point out that, from the construction of ω_ℓ as recalled in Appendix A, Eq. (A5) can be naturally generalized as

$$\mathbb{E}\left[e^{\sum_{m=1}^q i p_m \omega_{\ell_m}(x_m)}\right] = e^{\sum_{j=1}^q \sum_{k=1}^j \alpha(j,k) \rho_{\max(\ell_k, \ell_j)}(x_k - x_j)} \tag{25}$$

for any sequence $0, \ell_1, \ldots, \ell_q < T$. From the expression (A4) of $\rho_\ell(t)$, it results that Eq. (4) can be extended as equality in law for processes of both space and scale variables: one has, $\forall r < 1, 0 < \ell \leqslant T$, and $u \in [0, T]$,

$$\omega_{r\ell}(su) \overset{\mathcal{L}'}{=} \Omega_r + \omega_\ell(u), \tag{26}$$

where $\overset{\mathcal{L}'}{=}$ means that the two processes have the same finite-dimensional distributions of any order as processes in the half plane (ℓ, u) and Ω_r is a random variable of the same law as $\omega_{rT}(u)$ independent of the process $\omega_\ell(t)$.

Let $r < 1$ and $a \ll T$. From Eq. (18), the rescaled version of the wavelet transform of $X(t)$ reads

$$\begin{aligned} W(rx, ra) &\simeq \int_{\kappa r a}^{ra} s^{H-2} ds \int_{rx-ra}^{rx+ra} e^{\omega_s(b)} K_{\varphi,\psi}\left(\frac{rx-b}{s}, \frac{ra}{s}\right) db \\ &= r^H \int_{\kappa a}^{a} s^{H-2} ds \int_{x-a}^{x+a} e^{\omega_{rs}(rb)} K_{\varphi,\psi}\left(\frac{x-b}{s}, \frac{a}{s}\right) db. \end{aligned}$$

Thanks to Eq. (26), we can thus establish the self-similarity of the wavelet transform of $X(t)$:

$$W(rx, ra) \overset{\mathcal{L}'}{=} r^H e^{\Omega_r} W(x,a). \tag{27}$$

From Eq. (27), the definition of Ω_r, and Eqs. (3) and (22), it results that, for all $a \leqslant T$, the wavelet structure functions

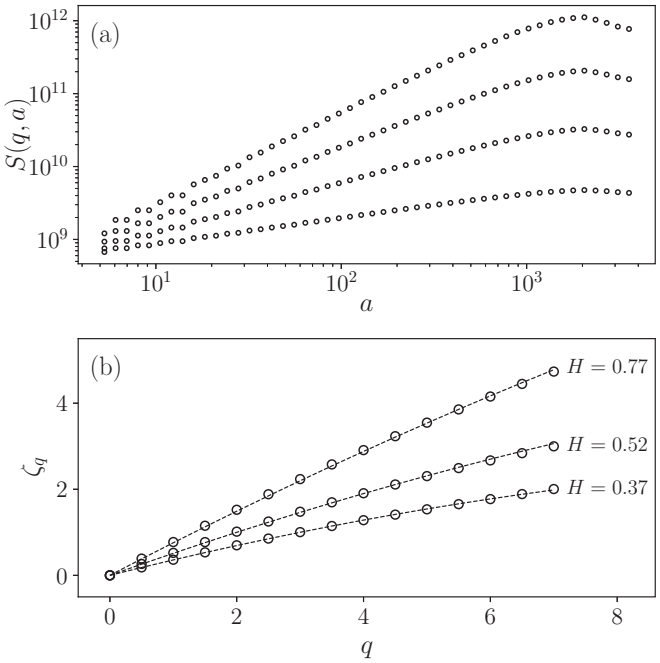

FIG. 3. Power-law scaling of structure functions of $X(t)$. In (a), the structure function $S(q,a)$ of $X(t,a)$ (with $H = 0.36$) is plotted in double logarithmic scale for $q = 1, 2, 3, 4$. The scaling range extents up to scales $a \sim 10^3$, which corresponds to the integral scale T. In (b), the estimated ζ_q (○) are compared to the expected log-normal expressions as given by Eq. (31) (dashed lines) for $H = 0.36$, 0.51, and 0.77 and $\lambda^2 = 0.025$.

are characterized by the multifractal scaling:

$$S(q,a) = \mathbb{E}[|W(x,a)|^q] = C_q\Big(\frac{a}{T}\Big)^{qH-\phi(q)} = C_q a^{\zeta_q}, \quad (28)$$

where $C_q = \mathbb{E}[|W(x,T)|^q]$. $X(t)$ has therefore multifractal properties in the sense that the absolute moments of its wavelet transform behave as a power law with a nonlinear concave multifractal spectrum ζ_q [38,40]. In particular, by considering Eq. (20), we deduce that the moments of absolute increments behave as power laws with the multifractal spectrum ζ_q:

$$\mathbb{E}[|X(t+a) - X(t)|^q] = C_q a^{\zeta_q}. \quad (29)$$

This result is illustrated in Fig. 3, where the estimated structure functions

$$S(q,a) = \sum_k |X(k+a) - X(k)|^q \quad (30)$$

are computed on realizations of log-normal versions of $X(t)$ with $H = 0.36$, 0.51, and 0.76, respectively, and $\lambda^2 = 0.025$. In each case, the integral scale has been set to $T = 2048$ and the overall sample length corresponds to 16 integral scales. In Fig. 3(a), we have plotted $\log_{10} S(q,a)$ as a function of $\log_{10} a$ in the case $H = 0.36$. We see that a power-law behavior extends from the smallest scale up to the integral scale. The estimated ζ_q spectrum, as obtained from a linear fit of these log-log plots, is reported in Fig. 3(b) (symbols ○). In the three cases, we obtain, with good precision, the expected scaling exponents:

$$\zeta_q = \Big(H + \frac{\lambda^2}{2}\Big)q - \frac{\lambda^2}{2}q^2, \quad (31)$$

represented by the dashed lines. Let us notice that in the case $H = 0.515$, one has $\zeta_2 = 2$ and therefore the successive increments of $X(t)$ are uncorrelated as in the Brownian motion (see next section). When $H = 0.36$ (precisely $H = 0.3585$), one has $\zeta_3 = 1$ as expected for the increments of the longitudinal velocity in fully developed turbulence [6].

It is well known that the spectrum of scaling exponents ζ_q can be, for a large class of functions, related to the singularity spectrum, i.e., the fractal (Haussdorf) dimension of the sets of iso-Hölder regularity [41–44]. This is the so-called multifractal formalism. At this stage, it is tempting to conjecture that the result proven by Barral and Seuret for random wavelet series [27] is also valid in the framework introduced here and that the multifractal formalism holds for continuous wavelet cascades. In our context, the Barral-Seuret result would say that $D(h)$, the singularity spectrum of $X(t)$, can be simply obtained from $D_M(\alpha)$, the singularity spectrum of the underlying log-infinitely divisible cascade $dM_t = \lim_{\ell\to 0} e^{\omega_\ell(t)}dt$. More precisely, if $D_M(\alpha)$ is the singularity spectrum of the continuous cascade $M(t)$ as provided by the multifractal formalism [44], i.e., in the range where $1 + \min_q[q\alpha - \phi(q)] > 0$, one has

$$D_M(\alpha) = 1 + \inf_q[q(\alpha-1) + \phi(q)]$$

and thus, from definition (23),

$$D_M(\alpha) = F(\alpha + H - 1). \quad (32)$$

Then the analog of the Barral-Seuret result (Theorem 1.1 of [27]) would assert that the singularity spectrum $D(h)$ of $\mathcal{W}$ cascades is provided by $D(h) = D_M(h+1-H)$, which according to (32) would simply mean that the singularity spectrum of $X(t)$ is $D(h) = F(h)$ in the range where $F(h)$, as given by (23), is positive. Since $F(h) = 1 + \inf_q(qh - \zeta_q)$ is the Legendre transform of the spectrum of the scaling exponents of wavelet transform structure functions, this would imply that the multifractal formalism holds for continuous $\mathcal{W}$ cascades.

B. Increment correlation functions and magnitude covariance

In this section, we study the behavior of various correlation functions associated with the increments (or wavelet coefficients) or the powers of their absolute values.

Let us first define the increment correlation function:

$$\begin{aligned}\rho(a,\tau) &= \mathbb{C}\mathrm{ov}(\delta_a X(t), \delta_a X(t+\tau)) \\ &= \mathbb{E}[\delta_a X(t)\delta_a X(t+\tau)]. \end{aligned} \quad (33)$$

It is easy to show that, when $a \ll \tau$, one has [45]

$$\rho(\tau) \simeq \frac{\partial}{\partial\tau}\tau^{-1}\mathbb{E}[\delta_\tau X(t)^2],$$

and therefore, from Eq. (29), one has

$$\rho(\tau) \simeq A\tau^{\zeta_2 - 2}. \quad (34)$$

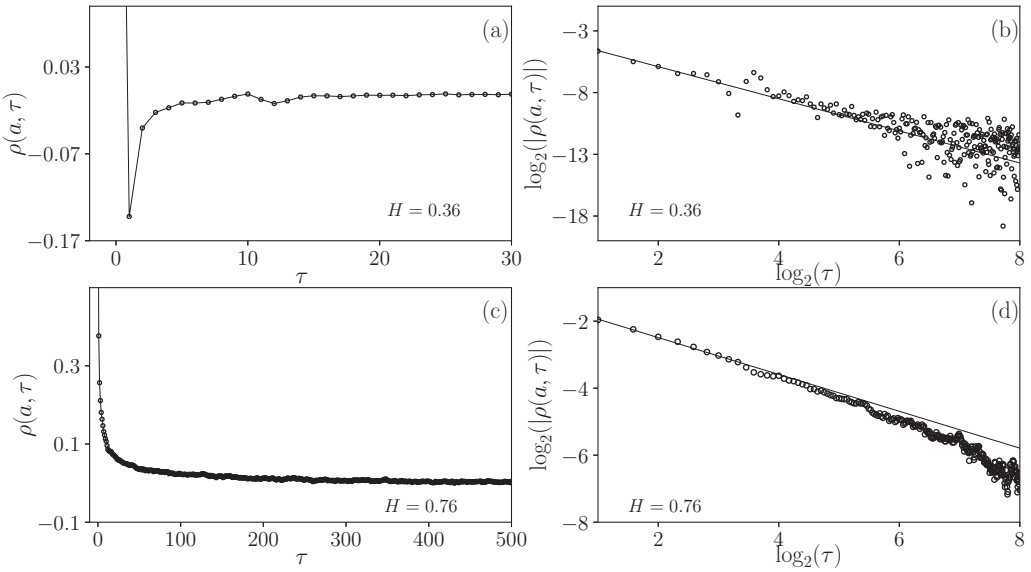

FIG. 4. Estimated correlation function of the increments of $X(t)$ for $H = 0.36$ [panels (a) and (b)] and $H = 0.76$ [panels (c) and (d)]. In both cases $\omega_\ell(t)$ is a Gaussian process of intermittency coefficient $\lambda^2 = 0.025$. The synthesizing wavelet $\varphi(t)$ is a "Mexican hat" wavelet, $g^{(2)}(t)$, defined in Eq. (15). As expected when H is small enough increments are anticorrelated while for H large enough they are positively correlated. The expected power-law behavior (34) is represented by the solid lines in panels (b) and (d).

Let us remark that if $\zeta_2 < 1$, then the prefactor A is negative and the increments are anticorrelated while if $\zeta_2 > 1$, the correlations are positive. This is reminiscent of the correlations of fractional Brownian motion [37,46] increments where $\zeta_2 = 2H$ and for which the value $H = 1/2$ separates the regimes of negatively and positively correlated fluctuations. The behavior (34) is illustrated empirically in Fig. 4 using two samples of $X(t)$ with respectively $H = 0.36$ and $H = 0.76$ while $\lambda^2 = 0.025$ and $T = 2048$ in both cases. The empirical increments correlation function have been estimated at scale $\tau = 1$ from samples of length 16 integral scales. As expected, one can observe, in Figs. 4(b) and 4(d), a power-law behavior in both cases and that $\zeta_2 - 2$ provides a good fit (solid lines). In Figs 4(a) and 4(c), we see that the process with $H = 0.36$, corresponding to $\zeta_2 = 0.695$, is characterized by anticorrelated increments while the one with $H = 0.76$, corresponding to $\zeta_2 = 1.495$, has positively correlated increments.

The behavior of the correlation function of the absolute power of the increments can be inferred from the self-similarity properties of the wavelet transform $W(x,a)$. The same kind of scaling argument as previously used to establish the scaling of structure functions can be used. Indeed, from Eq. (27), one has, for $a \leqslant \tau \leqslant T - \kappa a$,

$$\mathbb{E}[|W(x_0, ra_0)|^q |W(x_0 + r\tau_0, ra_0)|^p] = r^{\zeta_{q+p}} \mathbb{E}[|W(x_0, a_0)|^q |W(x_0 + \tau_0, a_0)|^p]. \quad (35)$$

Let us now choose $\varepsilon \ll 1$ and set $T' = \frac{T}{1+\varepsilon}$. Let us consider $ra_0 = a$, $r\tau_0 = \tau$, and $a = \varepsilon\tau$. The previous equation can be rewritten as

$$\mathbb{E}[|W(x_0, a)|^q |W(x_0 + \tau, a)|^p] = \left(\frac{\tau}{T'}\right)^{\zeta_{q+p}} \mathbb{E}[|W(x_0, \varepsilon T')|^q |W(x_0 + T', \varepsilon T')|^p]. \quad (36)$$

If one considers $\varepsilon \to 0$ (i.e., one chooses a very small), then $T' \simeq T$ and $W(x_0, \varepsilon T')$ becomes independent from $W(x_0 + T', \varepsilon T')$, and one has

$$\begin{aligned}\mathbb{E}[|W(x_0, \varepsilon T')|^q |W(x_0 + T', \varepsilon T')|^p] &\simeq \mathbb{E}[|W(x_0, \varepsilon T')|^q] \mathbb{E}[|W(x_0 + T', \varepsilon T')|^p] \\ &\sim K_{p,q}(a) \left(\frac{\tau}{T}\right)^{-\zeta_q - \zeta_p}, \end{aligned} \quad (37)$$

where $K_{p,q}(a)$ is a constant that depends on a. Given the scaling (29), this entails, for a fixed small value of a,

$$\mathbb{E}[|W(x_0, a)|^q |W(x_0 + \tau, a)|^p] \sim K_{p,q}(a) \left(\frac{\tau}{T}\right)^{\zeta_{p+q} - \zeta_q - \zeta_p}, \quad (38)$$

showing that correlation functions of the powers of the wavelet transform absolute value behave, at a given scale, as a power law as a function of the time lag τ with a scaling exponent $\zeta_{p+q} - \zeta_p - \zeta_q$. It is important to notice that this exponent does not depend on H and is only provided by the $\phi(q)$ nonlinear part of ζ_q.

This behavior is illustrated in Fig. 5, where we have plotted the estimation of absolute increments (i.e., in the case $p = q = 1$) for the two log-normal processes with $H = 0.36$ and $H = 0.77$ considered previously. As expected both behave, independently of H, as $\tau^{\zeta_2 - 2\zeta_1}$, which corresponds, according to Eq. (31), to the power law $\tau^{-\lambda^2}$ [represented by the dashed line in Fig. 5(b)].

Equation (38) can be used to compute the behavior of magnitude covariance as defined in Refs. [13,14]. Indeed, since

$$\mathbb{C}\mathrm{ov}(\ln|W(x_0, a)|, \ln|W(x_0 + \tau, a)|) = \left.\frac{\partial_q \partial_p \ln \mathbb{E}[|W(x_0, a)|^q |W(x_0 + \tau, a)|^p]}{\partial p \partial q}\right|_{q,p=0}, \quad (39)$$

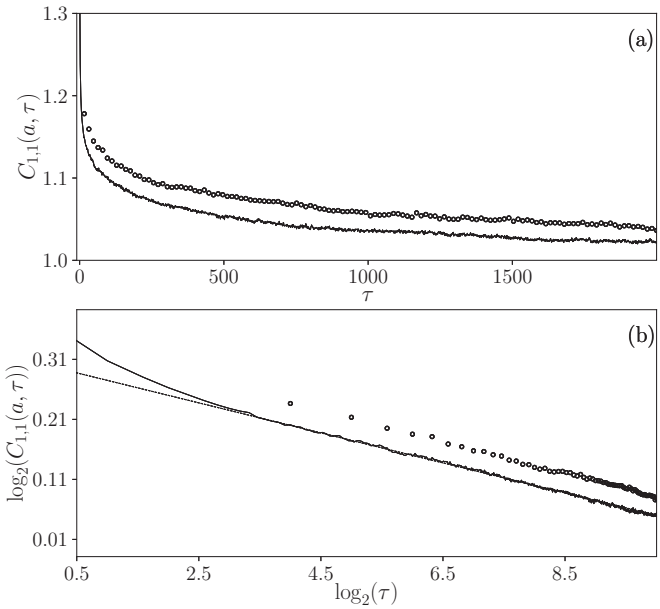

FIG. 5. Estimated correlation function of the absolute increments of $X_{LN}(t)$ for $H = 0.37$ (○) and $H = 0.77$ (solid lines) in (a) linear and (b) double logarithmic scales. As expected they both behave as $\tau^{-\lambda^2}$ independently of H [represented by the dashed line in (b)].

we obtain the well-known logarithmic magnitude covariance for multifractal processes [13,14]:

$$\mathbb{C}\mathrm{ov}(\ln|W(x_0,a)|, \ln|W(x_0+\tau,a)|) \simeq \zeta''(0)\ln\left(\frac{\tau}{T}\right) = -\lambda^2 \ln\left(\frac{\tau}{T}\right), \tag{40}$$

where we defined the intermittency coefficient as $\lambda^2 = -\zeta''(0)$.

V. SKEWNESS AND LEVERAGE EFFECT: APPLICATIONS TO TURBULENCE AND STOCK MARKET DATA

A. Skewness of increment pdf's at all scales

Because of the self-similarity relationship (27), one can also expect a scaling of odd moments of the wavelet transform, i.e., $\forall k \in \mathbb{N}, \forall a \leqslant T$,

$$S^\star(2k+1,a) = \mathbb{E}[W(x,a)^{2k+1}] = V_{2k+1}\, a^{\zeta_{2k+1}}. \tag{41}$$

This shows in particular that generically, the skewness

$$\mathcal{S}(a) \overset{\text{def}}{=} \frac{\mathbb{E}[W(x,a)^3]}{\mathbb{E}[W(x,a)^2]^{3/2}} \sim a^{\zeta_3-\frac{3}{2}\zeta_2} \tag{42}$$

increases (in absolute value) when $a \to 0$. The computation of the constant V_{2k+1} for a given wave form φ is tedious and can only be written as an intricate multiple integral, but it can be shown it is nonzero unless φ satisfies very specific conditions (see Fig. 8). The problem of studying the precise relationship between the synthesizing wavelet features and the values of constants V_{2k+1} or the questions related to a precise calibration of the skewness using experimental data is left as a prospect for a future work. In this section our goal is simply to illustrate, using basic examples, in which respect $\mathcal{CW}$ cascades are able to reproduce at least qualitatively experimental observations notably for longitudinal velocity increments in turbulence or return fluctuations of financial time series.

Previous considerations suggest that our approach, unlike constructions based on classical random measures, generically leads to skewed multifractal processes with a skewness that, like the flatness, increases as one goes from coarse to fine scales. This property and the scaling behavior (42) are illustrated in Fig. 6, where we have displayed the skewness $\mathcal{S}(a)$ of the increment distribution estimated at different scales for a log-normal $\mathcal{CW}$ cascade $X(t)$ that is antisymmetric by time reversal. We see that this skewness goes from $\mathcal{S} \simeq -0.5$ at large scales to $\mathcal{S} < -1$ at finer scales. In this example $X(t)$ was built using $\varphi = g^{(1)}$, the first derivative of the Gaussian function, $H = 0.36$, and ω_ℓ corresponding to a log-normal cascade with $\lambda^2 = 0.025$ and integral scale $T = 2^{12}$. In that respect, according to Eq. (31), $\zeta_3 = 1$ and $X(t)$ was designed to mimic the main features of velocity records in experiments of fully developed turbulence. All the estimations have been performed on a sample of length 128 integral scales. We see that our model not only provides a good fit of the scaling behavior of the increment absolute moments (as illustrated in Fig. 3) but also provides the correct order of magnitude of the skewness across scales as usually observed for the longitudinal velocity increments in turbulence [6] [see also Fig. 7(a) and Figs. 9(a) and 9(c) below].

The scaling relationship (41) indicates that the skewness will be zero at all scales if it vanishes at the largest scale T. It is noteworthy that this may be the case if the synthesizing wavelet φ in Eq. (9) is an even or odd function. Indeed, if the wavelet $\varphi(t)$ is a symmetric function, because $\omega_\ell(t) \overset{\mathcal{L}}{=} \omega_\ell(-t)$, we see from definition (9) that $X_\ell(t)$ is invariant by time reversal, i.e., one has $X_\ell(-t) \overset{\mathcal{L}}{=} X_\ell(t)$. It thus results that if the analyzing wavelet is an odd function [as, e.g., for the increments $\delta_\tau X(t)$] the wavelet transform of $X(t)$ will have a symmetric law implying that all odd moments are zero. In order to observe some skewness in the increment law, it is thus necessary to consider nonsymmetric synthesizing wavelets φ. Along the same line, if the synthesizing wavelet $\varphi(t)$ is antisymmetric, then $X(t)$ is odd by time reversal, i.e., $X_\ell(-t) \overset{\mathcal{L}}{=} -X_\ell(t)$, and if the analyzing wavelet is even [as, e.g., when one computes the second-order increments of $X(t)$, $\delta_\tau^{(2)}X(t) = X(t+2\tau) + X(t) - 2X(t+\tau)$], the wavelet transform will have a symmetric law. This means that if a skewness is observed in both first- and second-order increments, the wavelet $\varphi(t)$ is neither an even nor an odd function.

These behaviors are illustrated in Fig. 7, where we have displayed the probability density functions (pdf's) of the first and second increments at different scales of two versions of log-normal continuous wavelet cascades $X(t)$ with the same parameters as in Fig. 6 but that are respectively antisymmetric and symmetric by time reversal. In the first case, we used $\varphi = g^{(1)}$ (as in Fig. 6) while in the second case $\varphi = g^{(2)}$ [see Eq. (15)]. All the probability density functions reported in Fig. 7 are standardized, i.e., represent the distribution of increments normalized by their root mean square. They are displayed in semilog scales and shifted so that large-scale distributions are below fine-scale ones. In that way, one can

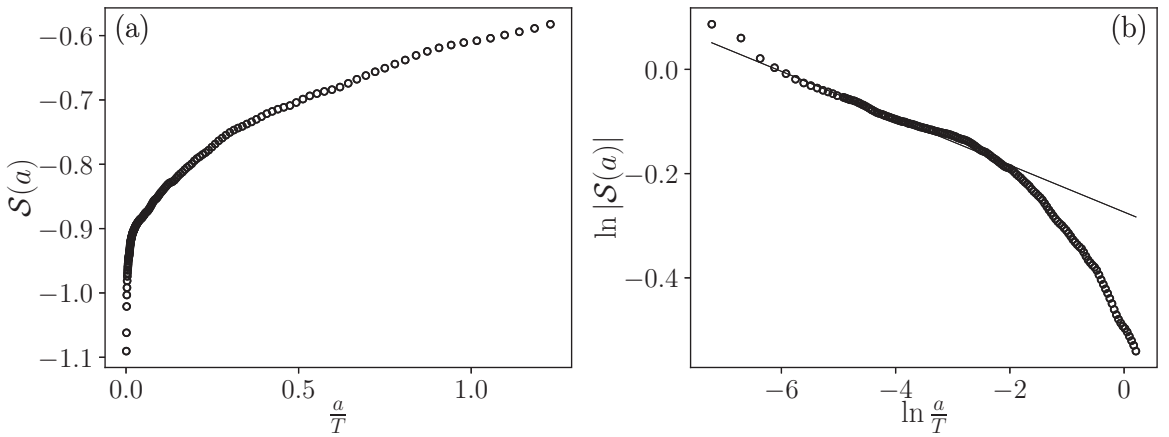

FIG. 6. Behavior of the estimated skewness $\mathcal{S}(a)$ [defined in Eq. (42)] as a function of the scale ratio $\frac{a}{T}$ for a log-normal $\mathcal{W}$ cascade of integral scale $T = 4096$, $\lambda^2 = 0.025$, and $H = 0.36$. The synthesizing wavelet is the odd function $g^{(1)}(t)$, the first derivative of the Gaussian function. The linear representation in (a) shows that $\mathcal{S}(a)$ takes values in the range $(-1.1, -0.6)$ for $\frac{a}{T}$ in the range $(10^{-3}, 1)$. In (b), the log-log representation allows one to check that the scaling $a^{\zeta_3-\frac{3}{2}\zeta_2}$ of Eq. (42) (solid line) provides a good fit to the data up to a scale $\frac{a}{T} \simeq 0.1$.

clearly observe the intermittency as an increasing of the flatness from large to small scales. We can check in panel (b) [resp. panel (c)] that if φ is odd (resp. even), the second (resp. first) order increments are symmetrically distributed. We can see in Fig. 7(a) that, at all scales, the increments of the antisymmetric version of $X(t)$ are negatively skewed (this

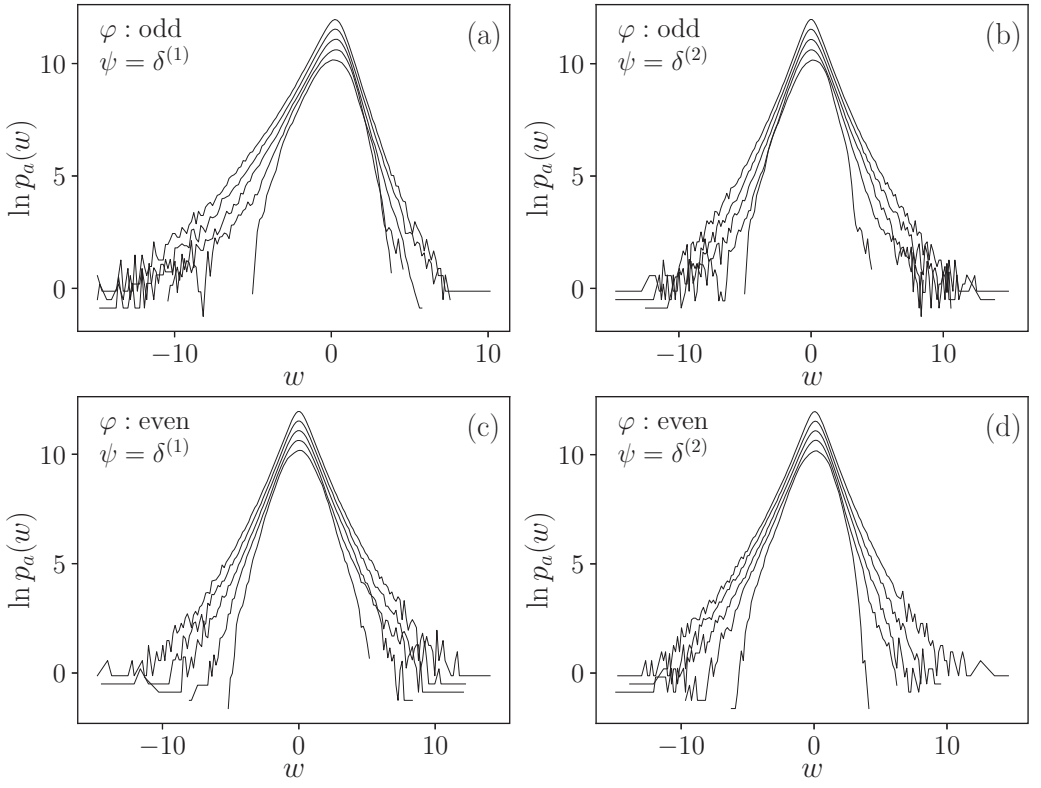

FIG. 7. Estimated "standardized" probability density function (pdf) of the "wavelet coefficients" at scale a, $p_a(w)$. At each scale, $a = T, \frac{T}{8}, \frac{T}{64}, \frac{T}{512}, \frac{T}{4096}$, where T stands for the integral scale, we have displayed $\ln p_a(w)$ up to an additive constant for the sake of clarity: pdf's at small scales are displayed above pdf's at coarser scales. In (a) and (b), the considered $\mathcal{W}$ cascade $X(t)$ is a log-normal process with a synthesizing wavelet φ that is an odd function [$g^{(1)}(t)$, the first derivative of the Gaussian function]. We can check that, due to the intermittency, the flatness increases from large to small scales. In (a) the analyzing wavelet is odd since it is $\psi(t) = \delta^{(1)}(t)$ [the one that corresponds to the increments of $X(t)$] while in (b) one uses $\psi(t) = \delta^{(2)}(t)$ and thus considers the second-order increments. As expected, one clearly observes, like in turbulence, skewed distributions of increments at all scales. The second-order increments are distributed with a symmetric law. In panels (c) and (d), the opposite effect is observed since the process $X(t)$ as been constructed using a symmetric wavelet, namely $g^{(2)}(t)$, the second-order derivative of the Gaussian function.

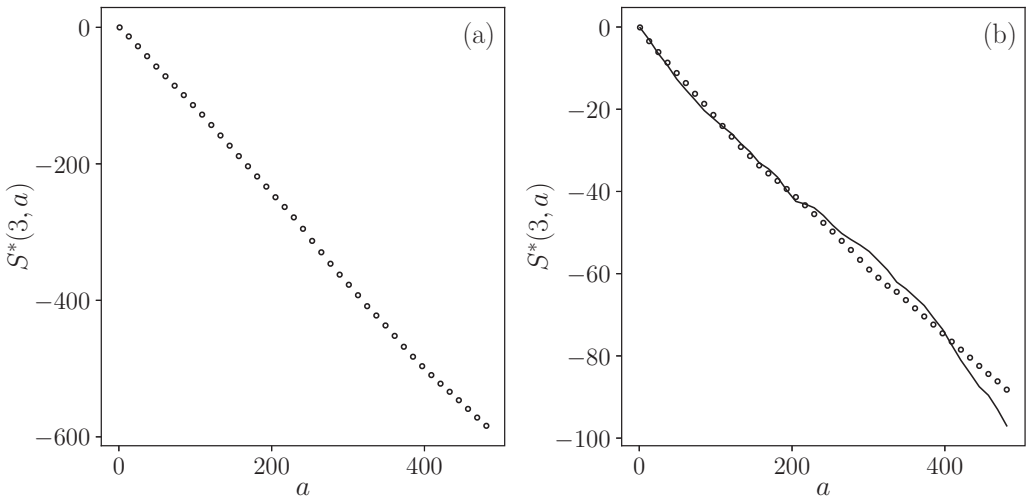

FIG. 8. Signed third-order structure function $S^*(3,a)$ as a function of the scale a. In (a), the mean order 3 moment of the increments is computed on $X(t)$ corresponding to the antisymmetric synthesizing wavelet $g^{(1)}(t)$ [Eq. (15)]. This confirms the (negative) skewness already illustrated in Fig. 7 and that, as expected for turbulence, $S^*(3,a)$ behaves as a linear function. In (b), $X(t)$ is built using the nonsymmetric wavelet depicted in Fig. 1(c). The third-order structure function behaves as a linear function and skewness can be observed for both first- (○) and second-order increments (solid line).

case corresponds to the plots of Fig. 6). The shapes of these skewed pdf's, with an increasing flatness, are strikingly similar to the distribution of longitudinal velocity increments in fully developed turbulence [47,48]. In the symmetric version of $X(t)$, the skewness is only observed on its second-order increments [Fig. 7(d)].

The fact that an antisymmetric synthesizing wavelet allows one to reproduce the observed skewness behavior of the velocity field, as illustrated in Fig. 6, can also be checked in the behavior of the signed third-order structure function. In Fig. 8, we have plotted, in linear scale, such signed structure function, $S^\star(3,a)$, as a function of the scale a estimated for

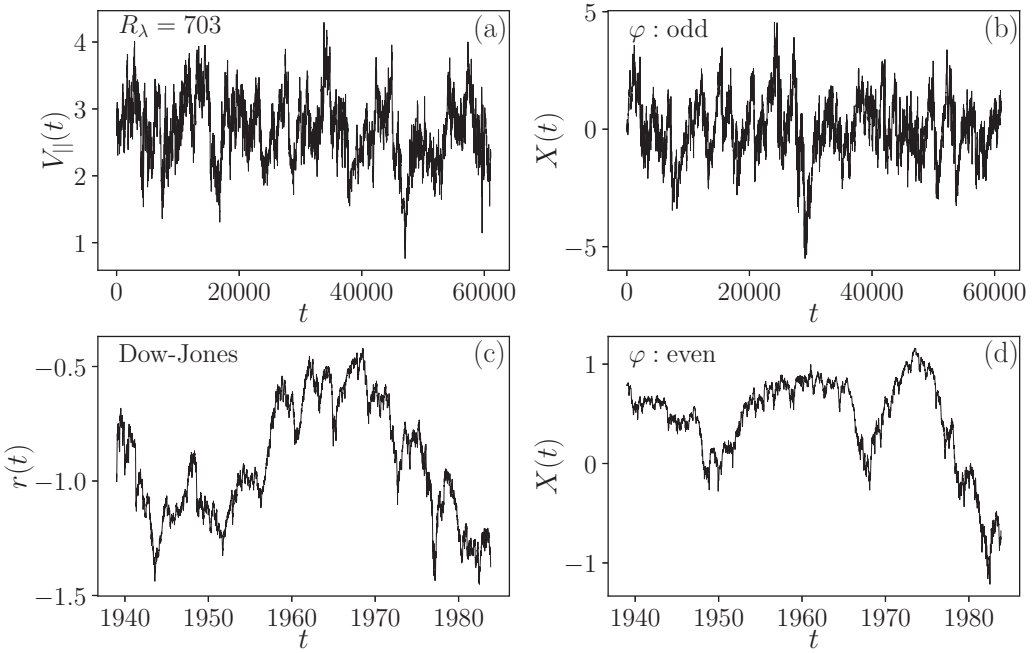

FIG. 9. Paths of turbulence velocity field and stock market data as compared to their $\mathcal{CW}$-cascade models. In (a) is represented the spatial fluctuation of the velocity component along the mean velocity direction (in m/s) as obtained in a high Reynolds number turbulence experiment ($R_\lambda \simeq 700$) realized by Castaing *et al.* [47]. Panel (b) corresponds to the cascade model obtained by fitting the turbulence multiscaling but also the skewness of law of first-order increments. In (c) is plotted the detrended daily variations of the logarithm of the Dow-Jones index over more than 4 decades (from 1939 to 1985). In (d) we have plotted a sample of its $\mathcal{CW}$-cascade model where we mainly account for the skewness of second-order increments. We can see that the "ramplike" behavior of turbulence data and "archlike" patterns of stock market data are remarkably well reproduced by $\mathcal{CW}$ cascades.

the log-normal $\mathcal{CW}$ cascade we used in Fig. 6 (i.e., calibrated to model the spatial fluctuations of the longitudinal velocity in turbulence with $\zeta_3 = 1$ and $\lambda^2 = 0.025$). It can be checked that for such a process we have $S^\star(3, a) = -Ka$. In full analogy with turbulence, one can wonder whether K could not be chosen such that, as in Kolmogorov theory, $K = \frac{4}{5}\varepsilon$, where ε is the mean dissipation rate $\varepsilon \sim \mathbb{E}[a^{-1}\nu \int_0^a dt\{\frac{\partial}{\partial t}X(t)\}^2]$ [6]. Since $X(t)$ is not differentiable, in order for this to be meaningful, we show, in Appendix E, that the so-called "dissipative anomaly" [49] property of the velocity field can be reproduced within our framework: if one chooses a "viscosity" $\nu(\ell)$ such that $\nu(\ell) \sim \ell^{4/3-\lambda^2}$, then

$$\lim_{\ell\to 0} \nu(\ell)\, \mathbb{E}\left[\left(\frac{\partial X_\ell(t)}{\partial t}\right)^2\right] = \varepsilon, \tag{43}$$

for some $0 < \epsilon < \infty$. Let us point out that it is likely that, from the definition Eq. (9), one could establish the following generalization of Eq. (43):

$$\nu(\ell)\left(\frac{\partial X_\ell}{\partial t}\right)^2 dt \underset{\ell\to 0}{\longrightarrow} \varepsilon(dt),$$

where $\varepsilon(dt)$ represents a singular measure corresponding to the multifractal dissipation [50] in the limit of vanishing viscosity and the convergence being interpreted in a weak sense.

Since the (negative) skewness of turbulence fields appears mainly on first-order increments (or on odd analyzing wavelets), as one can see in Figs 9(a) and 9(b), it can be directly visualized as "ramplike" (i.e., a slow increase followed by a rapid fall) patterns on the velocity profile and its model. This behavior is very different from the "archlike" shapes that can be associated with the negative skewness of the second-order increments. Such a feature is obviously present in the fluctuations of market prices as illustrated in the example of the Dow-Jones index in Fig. 9(c). In Figs 9(b) and 9(d), we plotted sample paths of log-normal models for respectively turbulence ($H = 0.36$, $\lambda^2 = 0.025$, and $\varphi = g^{(1)}$) and stock market data ($H = 0.51$, $\lambda^2 = 0.025$, and $\varphi = g^{(2)}$).

A close inspection of the Dow-Jones evolution in Fig. 9(c) reveals that this process has not only skewed second-order increments but also displays skewed first-order increments. Indeed, it is well known that financial return variations are characterized by rapid large drops that are followed by slower upward moves. It thus results that, in order to model the dynamics of market prices, a $\mathcal{CW}$ cascade should involve a wavelet that is neither odd nor even. In Fig. 8(b), we have computed the behavior of $S^\star(3, a)$ as a function of a for both first- and second-order increments when the wavelet is the nonsymmetric wavelet displayed in Fig. 1(c) (the other parameters are those chosen for turbulence). We see that both types of increments are characterized by a skewness of comparable magnitude since one observes third-order moments behave as similar linear functions of the scale. As discussed below, asymmetric synthesizing wavelets allow one to account for another feature observed on stock market data, namely the leverage effect.

B. Leverage effect

The fact that the synthesizing wavelet $\varphi(t)$ has no particular symmetry can be reflected by different statistical quantities. As discussed notably by Pommeau [51], there exists a wide variety of correlation functions that allow one to reveal the lack of time-reversal symmetry of a process $X(t)$. The "leverage" function is a particular example of such a measure. It consists of computing the correlation between the increments at some scale and their "amplitude" (e.g., their absolute value and their squared value) after or before some time lag τ [21,22,52]:

$$\mathcal{L}_q(\tau) = Z_{q,\ell}^{-1}\mathbb{E}[\delta_\ell X(t)|\delta_\ell X(t+\tau)|^q], \tag{44}$$

where $Z_{q,\ell}^{-1}$ is a properly chosen normalization constant: for example, in Ref. [52], the authors studied $\mathcal{L}_2$ with $Z_{2,\ell} = \mathbb{E}[\delta X_\ell^2]^2$. In general one will consider the behavior in the small-scale regime, i.e., the limit $\ell \to 0$ with a well-chosen normalization. The so-called "leverage effect" is a property that has been empirically observed on stock prices and stock market indices indicating that past returns are (negatively) correlated with future volatility [i.e., $\mathcal{L}_q(\tau) < 0$ for $\tau \geqslant 0$] while the reverse is not true [$\mathcal{L}_q(\tau) \simeq 0$ for $\tau < 0$]. In that context "returns" means increments of log-price while "volatility" stands for squared or absolute returns. The leverage effect can be intuitively explained by the fact that, after a large price drop, some kind of panic takes place with a large uncertainty and thus a large volatility results. The symmetric situation, i.e., a large upward price move, does not induce any crisis and therefore does not trigger any noticeable volatility variation.

Different attempts to account for this effect within the standard class of econometric models have been proposed [52,53]. Since the class of multifractal random walk as described in Sec. II A remarkably accounts for many of "stylized facts" of asset fluctuations, some authors considered different variants of these models that break the time-reversal symmetry by introducing specific correlations between cascade and noise terms [21,22]. But as mentioned in the introductory section, such approaches cannot lead to well-defined continuous time limits unless the noise has long-range correlations [22,23,54]. Since continuous $\mathcal{W}$ cascades are generically not invariant by time reversal one expects that it should be possible to account for the leverage effect by a specific choice of the synthesizing wavelet φ. According to the definitions (44) and (9), $\mathcal{L}_q(\tau)$ can be expressed as an intricate integral. In Appendix F, we show, using some heuristic approximations, that when $q = 1$, the leverage function behaves as

$$\mathcal{L}_1(\tau) \underset{\tau\gg\ell}{\sim} C_+|\tau|^{H-1-\phi(2)},$$
$$\mathcal{L}_1(\tau) \underset{\tau\ll-\ell}{\sim} C_-|\tau|^{H-1-\phi(2)},$$

where both scaling laws are valid in the range $|\tau| \ll T$. We have shown that the prefactors C_+ and C_- depend on the synthesizing wavelet φ as

$$C_+ = -\int_0^{+\infty} s^{H-1}ds \int du\varphi(u)C_s'(su+1),$$
$$C_- = -\int_0^{+\infty} s^{H-1}ds \int du\varphi(u)C_s'(su-1),$$

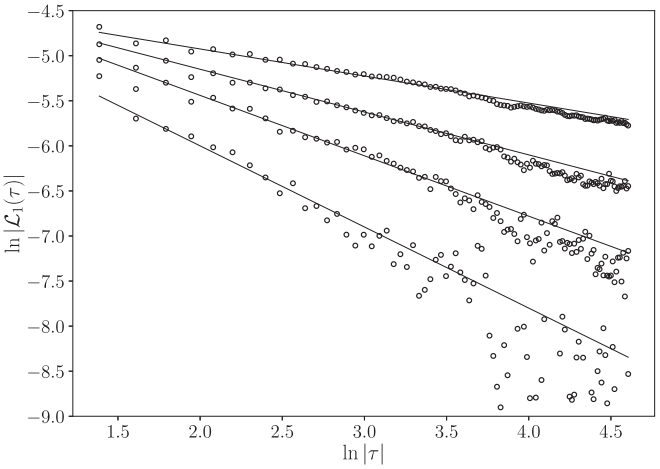

FIG. 10. Scaling of the leverage function. Estimated curves $|\mathcal{L}_1(\tau)|$ are plotted as a function of $|\tau|$ in double logarithmic scale [symbols (○)]. The estimations have been performed on samples of length $L = 2^{17}$ of log-normal $\mathcal{CW}$ cascades with $\lambda^2 = 0.025$, $T = 2^{10}$, and, from top to bottom, $H = 0.7$, 0.51, 0.33, and 0.1. The solid lines represent the corresponding theoretical power laws of exponent $H - 1 - \phi(2)$.

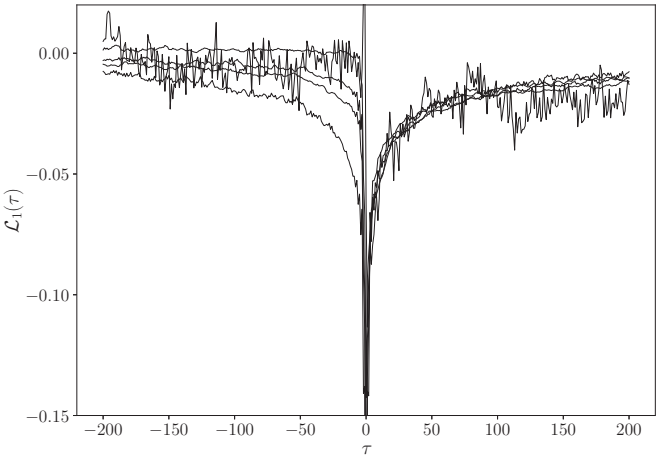

FIG. 11. Leverage functions $\mathcal{L}_1(\tau)$ estimated for a log-normal $\mathcal{CW}$ cascade with $H = 0.515$ and $\lambda^2 = 0.025$ (solid lines). The various curves correspond to different asymmetry factors α in the synthesizing wavelet defined in Eq. (46), namely $\alpha = \frac{1}{8}, \frac{1}{3}, \frac{1}{2}$, and 1. One sees that the behavior at lags $\tau > 0$ does not depend on α whereas the leverage function at negative lags becomes smaller and smaller as the asymmetry increases. For comparison purposes, the estimated leverage function from daily Dow-Jones index data is also reported (gray curve).

with $C_s(z) = \mathbb{E}[e^{\omega_s(t)+\omega_s(t+z)}]$. This scaling law is illustrated in Fig. 10, where we have checked, using estimations from simulated data, that it holds for different values of H in the case of a log-normal cascade built with an antisymmetric wavelet. Notice that from the previous expression, C_- and C_+ are not necessarily equal and the leverage effect could therefore be observed when the leverage ratio

$$\kappa = \frac{C_+}{C_-} \tag{45}$$

is very large (i.e., $\kappa \gg 1$).

For illustration purposes and in order to handle reasonable expressions, let us consider the "simple" case when $\varphi(t)$ is a piecewise constant function:

$$\varphi(t) = \alpha^{-1}\mathbb{I}_{[0,\alpha)}(t) - \mathbb{I}_{[-1,0)}(t), \tag{46}$$

where $0 < \alpha < 1$ controls the wavelet asymmetry.

In Fig. 11 we have plotted the leverage function estimated from numerical simulations of log-normal $\mathcal{CW}$ cascades with a synthesizing wavelet corresponding to Eq. (46) with different asymmetry factors $\alpha = 1/8, 1/3, 1/2$, and 1. We chose $T = 2^{13}$, $\lambda^2 = 0.025$, and $H = 0.51$ so that the increments are uncorrelated ($\zeta_2 = 1$). We first clearly see that the behavior for positive lags appears to not depend on α while the situation is very different for negative lags: as α decreases one sees that the leverage function lessens more and more. One goes from a symmetric leverage function in the case $\alpha = 1$ to a situation where it is almost zero at negative lags. This latter case is very interesting to reproduce the empirical features observed in the stock market; for comparison we have plotted the leverage function estimated from the Dow-Jones index daily returns over a period extending from 1939 to 2018 (gray line in Fig. 11). These empirical findings show that the leverage ratio strongly depends on α and becomes arbitrarily large when α is small. Even if it is possible to show that the constants $C_\pm$ are bounded in the case when φ is defined by Eq. (46), their exact value can however hardly be obtained or approximated under a closed form. We then estimated them by means of a numerical integration. The so computed leverage ratios are reported in Fig. 12. In the case when $\alpha = 1$, we naturally recover the fact that the leverage effect is not present while we observe that κ strongly increases for small α. Notice that

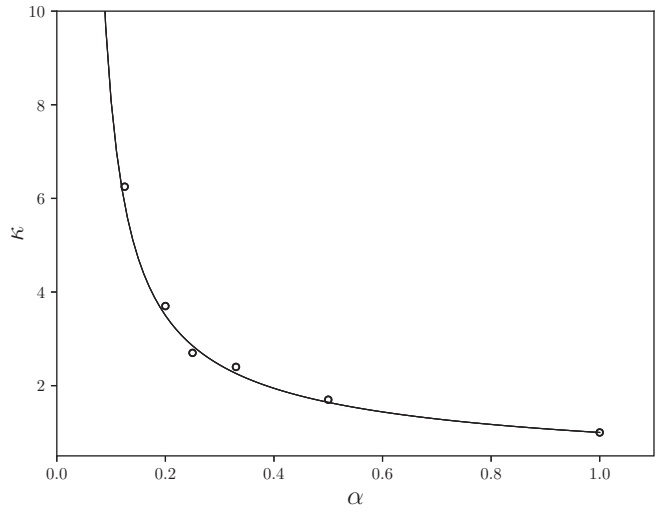

FIG. 12. Evolution of the leverage ratio κ [Eq. (45)] as a function of the coefficient α characterizing the asymmetry of the synthesizing wavelets defined in Eq. (46). The numerical integrations have been performed in the log-normal case with $\lambda^2 = 0.025$ and $H = 1/2 + \lambda^2$. The symbols (○) represent the value of κ as estimated from the empirical leverage function obtained from simulated data of length $128T$ with $T = 2^{13}$.

our numerical estimations confirm that both C_+ and C_- are negative in the range $0.1 \leqslant \alpha \leqslant 1$. We also observed that C_+ is almost independent of α while C_- becomes arbitrarily small as $\alpha \to 0.048$, where it changes its sign. It thus seems possible, within this model, to obtain a "perfect" leverage effect with an infinite leverage ratio corresponding to a vanishing leverage function in the domain $\tau < 0$. These numerical computations of the leverage ratio have been checked using empirical estimation from numerical simulations (symbols $\circ$).

VI. SUMMARY AND PROSPECTS

In this paper we have proposed a way to build random multifractal functions with stationary increments, exact scaling, and self-similarity properties. Our model simply consists of extending former $\mathcal{W}$ cascades by replacing the framework of an orthogonal wavelet basis with that of a continuous wavelet transform and the discrete multiplicative weights with their log-infinitely divisible counterpart, i.e., the process $e^{\omega_\ell(t)}$ involved in the construction of continuous cascade measures. We have shown that our construction provides almost surely Lipschitz regular paths and studied its self-similarity and scaling properties. As emphasized in Sec. V, $\mathcal{CW}$ cascades are in general skewed multifractal processes and are characterized by a nonsymmetric correlation between increment signs and amplitudes (the so-called "leverage effect"). For model calibration purpose, it remains to study how to quantitatively relate the skewness values to the synthesizing wavelet properties. As far as applications to turbulence are concerned, since our framework can easily reproduce the skewed intermittency phenomenon observed for the velocity fluctuations, together with the dissipative anomaly, it provides undoubtedly a promising way to account for many stochastic aspects of fluid dynamics in regimes of fully developed turbulence. It that respect, vector and 3-dimensional extensions of $\mathcal{CW}$ cascades with the possibility of introducing well-known dynamical properties such as incompressibility (as, e.g., in Refs. [55,56]) could be interesting in order to get a more realistic model.

Beyond applications to specific contexts and the previously mentioned problems, a fundamental question is to know which features of the synthesizing wavelet remain observable through the associated continuous cascade. Is there a analog of the famous black holes "no-hair theorem" [57] in the present framework? This "inverse problem" is interesting since we already know that some important properties such as skewness, the behavior of the leverage function, and the prefactor values in scaling relationships may depend on the specific wavelet shape, but the issue is to precisely know in what respect and also which properties of φ (such as the number of vanishing moments and the moment values) can be recovered from empirical data.

Finally, let us mention that, by simply replacing $e^{\omega_\ell(t)}$ by its lacunary version introduced in Ref. [58], our framework may also allow one to build random functions that are almost everywhere smooth and singular on random Cantor sets. One could also slightly extend the definition of $\mathcal{CW}$ cascades in order to build a stationary variant of the class of lacunary wavelet series that possess oscillating singularities defined and studied by Arneodo *et al.* [28,29]. Such processes are not self-similar but possess a self-similar wavelet transform. All these prospects will be considered in a future work.

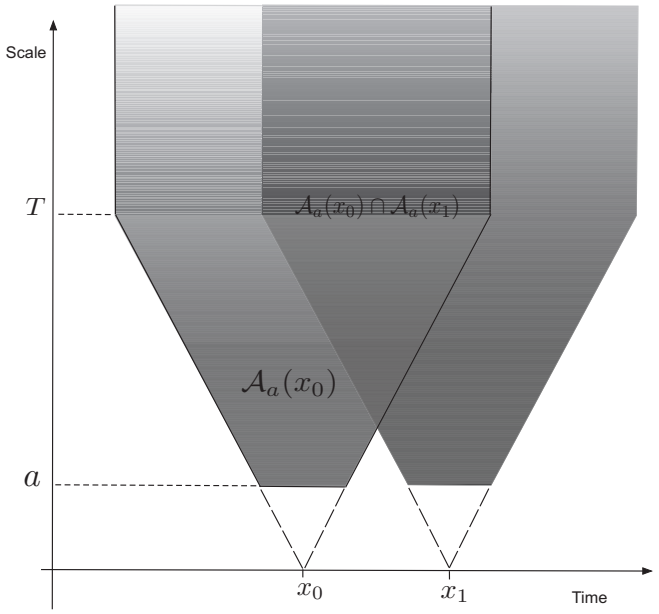

FIG. 13. The domains $\mathcal{A}_a(x_0)$ and $\mathcal{A}_a(x_1)$ and their intersection.

APPENDIX A: CONTINUOUS CASCADE CONSTRUCTION

The process $\omega_\ell(x_0)$ in the definition (2) is constructed as follows: On considers the time scale half plane $(t, s) \in \mathbb{R} \times \mathbb{R}^{+*}$ and the natural measure $dm(t, s) = s^{-2}dtds$, which gives the area of any set $\mathcal{S}$ as

$$|\mathcal{S}| = \int_{\mathcal{S}} dm(t, s) = \int_{\mathcal{S}} s^{-2}dtds.$$

Within this framework, one considers $dP(t, s)$ a random infinitely divisible "white noise" (the so-called "independently scattered random measure") such that the measure of a given set $\mathcal{S}$, $P(\mathcal{S}) = \int_{\mathcal{S}} dP(t, s)$, is an infinitely divisible random variable of characteristic function

$$\mathbb{E}[e^{ikP(\mathcal{S})}] = e^{|\mathcal{S}|\phi(ik)}, \tag{A1}$$

where $\phi(q)$ is the cumulant generating function associated with an infinitely divisible law as provided by the celebrated Levy-Khintchine theorem [32]. For example, if $\phi(q) = qH - \lambda^2 q^2/2$, $dP(t, s)$ is simply a Gaussian white noise of mean $Hs^{-2}dtds$ and variance $\lambda^2 s^{-2}dtds$.

Let us now, as in Refs. [11,12], consider $dP(t, s)$ such that $\phi(1) = 0$ and define, for any $T > 0$, the conelike domain $\mathcal{A}_a(x_0)$ as

$$(x, s) \in \mathcal{A}_a(x_0) \Leftrightarrow \{s \geqslant a,\ 2|x - x_0| \leqslant \min(s, T)\}. \tag{A2}$$

The shape of $\mathcal{A}_a(x_0)$ is depicted in Fig. 13. The process $\omega_\ell(x)$ is then simply defined as

$$\omega_\ell(x) = P[\mathcal{A}_\ell(x)]. \tag{A3}$$

Let $\rho_\ell(\tau)$ be the area of the set $\mathcal{A}_\ell(x_0) \cap \mathcal{A}_\ell(x_0+\tau)$ (see Fig. 13). A direct computation leads to

$$\rho_\ell(\tau) = \begin{cases} \ln\left(\frac{T}{\ell}\right) + 1 - \frac{\tau}{\ell}, & \text{if } \tau \leqslant \ell, \\ \ln\left(\frac{T}{\tau}\right), & \text{if } T \geqslant \tau \geqslant \ell, \\ 0, & \text{if } \tau > T. \end{cases} \tag{A4}$$

In Ref. [12] it is shown that the characteristic function of $\omega_\ell(x)$, for any $q \in \mathbb{N}^*$, $(x_1, x_2, \ldots, x_q) \in \mathbb{R}^q$ with $x_1 \leqslant x_2 \leqslant \ldots \leqslant x_n$, and $(p_1, p_2, \ldots, p_q) \in \mathbb{R}^q$, is given by

$$\mathbb{E}\left[e^{\sum_{m=1}^q i p_m \omega_\ell(x_m)}\right] = e^{\sum_{j=1}^q \sum_{k=1}^j \alpha(j,k)\rho_\ell(x_k - x_j)}, \tag{A5}$$

where $\alpha(j,k)$ are coefficients defined in Ref. [12] that satisfy

$$\sum_{j=1}^q \sum_{k=1}^j \alpha(j,k) = \phi\left(\sum_{k=1}^q p_k\right). \tag{A6}$$

Expression (A5) entails in particular that $\rho_\ell(\tau)$ corresponds to the covariance (when it exists) of $\omega_\ell(x)$ and $\omega_\ell(x+\tau)$. Notably, in the case when $dP(t,s)$ is a Gaussian white noise, the above construction of $e^{\omega_\ell(t)}$ is an example of the celebrated Kahane multiplicative chaos measure [59,60] and corresponds to the measure originally proposed in the MRW construction [14,17].

APPENDIX B: WEAK CONVERGENCE OF $X_{2^{-n}}(t)$ IN THE SPACE OF CONTINUOUS FUNCTIONS

Let us show that the series

$$X^{(n)}(t) = X_{2^{-n}}(t) = \int_{2^{-n}}^T s^{H-2} ds \int_{-\infty}^{+\infty} e^{\omega_s(b)} \varphi\left(\frac{t-b}{s}\right) db \tag{B1}$$

converges in the weak sense when $n \to \infty$ in the space of continuous functions.

We first need a result that can be found, e.g., in Ref. [58] that can be directly deduced from the definition of $\omega_s(t)$ in Appendix A: for all $s' \leqslant s \leqslant T$, one has

$$\mathbb{E}[e^{\omega_s(u)+\omega_{s'}(v)}] = e^{[\phi(2)-2\phi(1)]\rho_s(u-v)+\phi(1)[\rho_s(0)+\rho_{s'}(0)]},$$

where $\rho_s(\tau)$ is defined in Eq. (A4). From this expression, one deduces

$$\mathbb{E}[e^{\omega_s(u)+\omega_{s'}(v)}] \leqslant C_1 s^{\phi(1)-\phi(2)} s'^{-\phi(1)},$$

i.e., assuming (10),

$$\mathbb{E}[e^{\omega_s(u)+\omega'_s(v)}] \leqslant C_1 s^{-\phi(2)}. \tag{B2}$$

Let us first show that all finite-dimensional distributions of $X^{(n)}$ converge. For that purpose it suffices to show that for all $m, n \to 0$,

$$\mathbb{E}[\{X^{(n)}(t) - X^{(m)}(t)\}^2] \to 0,$$

and therefore, assuming $n \leqslant m$,

$$\mathbb{E}\left[\left\{\int_{2^{-m}}^{2^{-n}} s^{H-2} ds \int_{-\infty}^{+\infty} e^{\omega_s(b)} \varphi\left(\frac{t-b}{s}\right) db\right\}^2\right] \to 0.$$

By permuting expectation and integration, we have to show that

$$\iint_{[2^{-m},2^{-n}]} ds_1 ds_2 (s_1 s_2)^{H-2} \iint db_1 db_2 \varphi\left(\frac{t-b_1}{s_1}\right) \times \varphi\left(\frac{t-b_2}{s_2}\right) \mathbb{E}[e^{\omega_{s_1}(b_1)+\omega_{s_2}(b_2)}] \to 0.$$

Since φ is bounded and supported by $[-1/2, 1/2]$, the previous expression can be bounded by

$$2C_2 \int_{2^{-m}}^{2^{-n}} ds_1 \int_{s_1}^{2^{-n}} ds_2 \, (s_1 s_2)^{H-2} \int_{-s_1/2}^{s_1/2} \times \int_{-s_2/2}^{s_2/2} db_1 db_2 \mathbb{E}[e^{\omega_{s_1}(b_1)+\omega_{s_2}(b_2)}]$$

and thus, thanks to (B2),

$$\mathbb{E}[\{X^{(n)}(t) - X^{(m)}(t)\}^2] \leqslant C_3 2^{-n[2H-\phi(2)]}.$$

$X^{(n)}(t)$ is therefore a Cauchy sequence provided

$$\phi(2) < 2H. \tag{B3}$$

In order to prove the weak convergence, it remains to establish the tightness of the sequence [61]. Since the sequence $X^{(n)}(t)$ is a continuous process, from [62], it suffices to show that

$$\sup_n \mathbb{E}[|X^{(n)}(t)|^\nu] < \infty \quad \text{and}$$

$$\sup_n \mathbb{E}[|X^{(n)}(t) - X^{(n)}(u)|^\beta] \leqslant C|t-u|^\gamma$$

for some positive ν, β, and γ. Let us show that both assertions hold for $\nu = \beta = 2$ if one supposes that (B3) is satisfied. In that case, by the same kind of computation as previously, thanks to inequality (B2), one can show that $\mathbb{E}[|X^{(n)}(t)|^2] \leqslant C$, where C does not depend on n. Moreover, we have

$$\begin{aligned} &\mathbb{E}[\{X^{(n)}(t) - X^{(n)}(u)\}^2] \\ &= \int_{2^{-n}}^T ds_1 \int_{s_1}^T ds_2 (s_1 s_2)^{H-2} \iint db_1 db_2 \, \mathbb{E}[e^{\omega_{s_1}(b_1)+\omega_{s_2}(b_2)}] \\ &\quad \times \left[\varphi\left(\frac{t-b_1}{s_1}\right) - \varphi\left(\frac{u-b_1}{s_1}\right)\right]\left[\varphi\left(\frac{t-b_2}{s_2}\right) \right. \\ &\quad \left. - \varphi\left(\frac{u-b_2}{s_2}\right)\right]. \end{aligned}$$

Let us choose γ such that

$$0 < 2\gamma < 2H - \phi(2). \tag{B4}$$

Then the last expression can be bounded provided $\varphi(t)$ belongs to the uniform Hölder space $C^\gamma(\mathbb{R})$, i.e., $\exists K_\gamma < \infty$ such that $\forall t, u$, $|\varphi(t) - \varphi(u)| \leqslant K_\gamma |t-u|^\gamma$. We thus have, using Eq. (B2) and condition (B4),

$$\mathbb{E}[\{X^{(n)}(t) - X^{(n)}(u)\}^2] \leqslant K'|t-u|^{2\gamma},$$

where

$$\begin{aligned} K' &= K_\gamma \int_0^T ds_1 \int_{s_1}^T ds_2 s_1^{H-1-\gamma} s_2^{H-1-\phi(2)-\gamma} \\ &= K_\gamma \frac{T^{2H-2\gamma-\phi(2)}}{(H-\gamma)[2H-2\gamma-\phi(2)]} \end{aligned}$$

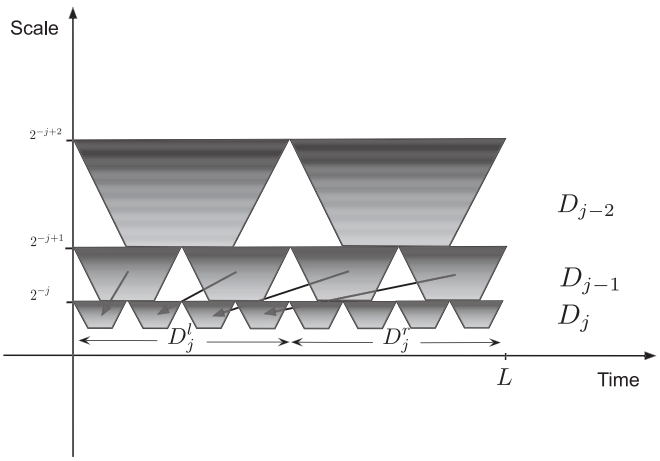

FIG. 14. The domains L_j involved in the proof of L^2 convergence. Each shaded domain represents a set $D(j,k)$, while L_j is the set of indices k for the $D(j,k)$ that cover the interval $[0,L]$.

does not depend on n. This ends the proof of the tightness of the sequence and thus establishes the weak convergence of the sequence $X^{(n)}$ towards a continuous process $X(t)$.

APPENDIX C: ALMOST SURE PATHWISE GLOBAL REGULARITY OF $X(t)$

Let us consider $h_{\min} > 0$ as defined in Eq. (C8). We then show that, for any $L > 0$, $X(t)$ has a uniform Lipschitz regularity α for all $\alpha < h_{\min}$ on $[0,L]$. For that purpose, we adapt the proof of Ref. [26] originally proposed for discrete $\mathcal{W}$ cascades on an orthogonal wavelet basis. Let $\psi_{j,k}(t) = 2^j\psi(2^jt-k)$ be a basis of $L^2([0,L])$ of compactly supported wavelets. For the sake of simplicity, we will not care about boundary wavelets and we will only consider wavelets $\psi_{j,k}$ that constitute a basis of $L^2(\mathbb{R})$ that support $S_{j,k}$ is such that $S_{j,k} \cap [0,L] \neq \emptyset$ (see, e.g., [25] for details about wavelet bases on an interval). We refer to L_j the set of indices k that satisfy this property. We can, without loss of generality, assume that $|S_{j,k}| = 2^{-j}$. Let $c_{j,k}$ be the wavelet coefficients $X(t)$:

$$c_{j,k} = \int \psi_{j,k}(t)X(t)dt. \tag{C1}$$

From expression (18), since the kernel K is bounded, $c_{j,k}$ can be controlled as

$$|c_{j,k}| \leqslant K2^{-jH} \sup_{t,s\in D(j,k)} e^{\omega_s(t)}, \tag{C2}$$

where $D(j,k)$ stands for the domain in the time scale plane $s \in [\kappa 2^{-j}, 2^{-j}]$, $t \in [2^{-j}k - \frac{s}{2}, 2^{-j}k + \frac{s}{2}]$ (these domains are depicted as shaded regions in Fig. 14).

In order control the regularity of $X(t)$, one can use a standard result in wavelet analysis: $X(t)$ is uniformly Lipschitz $\alpha < 1$ over $[0,L]$ if and only if there exists a uniform constant C and some integer $0 \leqslant J < \infty$; thus,

$$|c_{j,k}| \leqslant C2^{-j\alpha}, \quad \forall j \geqslant J, \quad k \in L_j. \tag{C3}$$

Let D_j be the time scale set D_j defined as (see Fig. 14)

$$D_j = \bigcup_{k\in L_j} D(j,k), \tag{C4}$$

and define

$$m_j = \sup_{(t,s)\in D_j} 2^{-jH}e^{\omega_s(t)}. \tag{C5}$$

From (C2) and (C3), we thus have to control the probability that $m_j > 2^{-j\alpha}$ in order to establish global Lipschitz regularity α of $X(t)$.

Let us suppose that $L = 2^M < T$, where T is the integral scale of $\omega_s(t)$; a proof for an arbitrary value of L can be easily adapted by splitting the interval into small pieces of size smaller than T. Let us now consider that $D_j = D_j^l \cup D_j^r$, where D_j^l and D_j^r are the union of the $D(j,k)$ for the 2^{M-1} values of k corresponding to respectively the first and the second half-part of L_j (see Fig. 14). Let $m_j^l = \sup_{(t,s)\in D_j^l} 2^{-jH}e^{\omega_s(t)}$ and $m_j^r = \sup_{(t,s)\in D_j^r} 2^{-jH}e^{\omega_s(t)}$. We have obviously $m_j = \max(m_j^l, m_j^r)$. By stationarity of the process $\omega_s(t)$, m_j^r and m_j^l have the same law. Moreover, from the construction of $\omega_s(t)$ as the integral of an infinitely divisible noise over a cone domain, they both can we written as X^lY and X^rY, where X^r and X^l have the same law, and X^l, X^r, and Y are independent. As shown in Ref. [26], it results that

$$\mathbb{P}[m_j \leqslant z] \geqslant \mathbb{P}\big[m_j^l \leqslant z\big]^2. \tag{C6}$$

Let us notice that one can map the domain D_{j-1} used to define m_{j-1} to the domains D_j^l by simply considering the scale and time dilation $s \to s/2$ and $x \to x/2$. Such a mapping is illustrated by the arrows in Fig. 14. Thus, from the self-similarity property of $\omega_s(t)$ [Eq. (4)], we have

$$\begin{aligned}\{2^{-jH}e^{\omega_s(t)}\}_{(t,s)\in D_j^l} &= \{2^{-jH}e^{\omega_{s/2}(t/2)}\}_{(t,s)\in D_{j-1}} \\ &\overset{\mathcal{L}}{=} 2^{-H}e^{\Omega_{1/2}}\{2^{-(j-1)H}e^{\omega_s(t)}\}_{(t,s)\in D_{j-1}},\end{aligned}$$

where $\Omega_{1/2}$ is a random variable independent of the process $\omega_s(t)$ such that

$$\mathbb{E}[e^{q\Omega_{1/2}}] = 2^{\phi(q)}.$$

This notably implies that

$$\mathbb{P}\big[m_j^l \leqslant z\big] = \mathbb{P}[2^{-H}e^{\Omega_{1/2}}m_{j-1} \leqslant z].$$

By recurrence we thus obtain

$$\mathbb{P}[m_j \leqslant z] \geqslant \mathbb{P}\big[m_0 2^{-jH}e^{\sum_{i=1}^j \Omega_{1/2}^{(i)}} \leqslant z\big]^{2^j},$$

where $\Omega_{1/2}^{(i)}$ are independent copies of $\Omega_{1/2}$. It thus results that

$$\begin{aligned}\mathbb{P}[m_j \geqslant z] &\leqslant 1 - \big(1 - \mathbb{P}\big[m_0 2^{-jH}\, e^{\sum_{i=1}^j \Omega_{1/2}^{(i)}} \geqslant z\big]\big)^{2^j} \\ &\leqslant 2^j \mathbb{P}\big[m_0 2^{-jH}\, e^{\sum_{i=1}^j \Omega_{1/2}^{(i)}} \geqslant z\big].\end{aligned} \tag{C7}$$

Let us now consider $z = 2^{-\alpha j}$ and set $W = 2^{-H} e^{\Omega_{1/2}}$. Then, provided

$$-\infty < \alpha < -\mathbb{E}[\log_2(W)] = H - \phi'(0),$$

according to Lemma 2 of Ref. [26] (relying on standard large deviation results), for any $\varepsilon > 0$, there exists $J_0 > 0$ such that, $\forall\ j > J_0$,

$$\mathbb{P}\left[m_0 2^{-jH} e^{\sum_{i=1}^{j} \Omega_{1/2}^{(i)}} \geqslant 2^{-\alpha j}\right] < e^{\varepsilon j} 2^{jF(\alpha)},$$

where $F(\alpha) = 1 + \inf_q(q\alpha - \zeta_q)$ with $\zeta_q = qH - \phi(q)$. Let us suppose that there exists $\eta > 0$ such that $F(\alpha) < 0$ in some interval $[0, \eta)$ and that

$$h_0 = H - \phi'(0) > 0.$$

Then by choosing $0 < \alpha < \eta$ we have, by combining previous inequality and inequality (C7),

$$\mathbb{P}[m_j \geqslant 2^{-\alpha j}] < e^{\varepsilon j} 2^{j[F(\alpha)+1]},$$

so one can choose ϵ small enough such that

$$\sum_j \mathbb{P}[m_j \geqslant 2^{-\alpha j}] < \infty,$$

which means, thanks to the Borel-Cantelli lemma, that almost surely there exists J such that $m_j < 2^{-\alpha j}$ for $j > J$. We directly deduce that, almost surely, $X(t)$ is a Lipschitz α function. We can therefore conclude that $X(t)$ is almost surely uniformly Lipschitz α for all $\alpha < h_{\min}$ with

$$h_{\min} = \sup\{h, F(h) < 0 \text{ and } h < H - \phi'(0)\}. \tag{C8}$$

APPENDIX D: SIMULATION METHOD

We provide some precision about the way we performed the numerical simulations used in the paper. Let $r > 0$ and define $\varepsilon_r[k]$ as an infinitely divisible noise defined such that

$$\mathbb{E}[e^{q\varepsilon_r[k]}] = e^{r\phi(q)}$$

with $\phi(1) = 0$. For instance, in the Gaussian case, $\phi(q) = \lambda^2 q(q-1)/2$ and, if ΔW_k represents an i.i.d. $N(0, \lambda^2)$ Gaussian white noise, then $\varepsilon_r[k] = \sqrt{r}\,\Delta W_k - r\lambda^2/2$.

Let $\theta_a(z)$ be the indicator function of the interval $[-a/2, a/2]$ and $\varphi_a(z) = \varphi(z/a)$ be the synthesizing wavelet at scale a. Let $\star$ stand for the (fast) discrete convolution operator. In order to generate a sample of $X_\ell(t)$ over an interval at sampling rate Δt, one considers a discrete version of Eq. (9):

$$X_\ell(k\Delta t) = \sum_{n=1}^{N} \Delta s_n\, s_n^{H-2} (\varphi_{s_n} \star e^{\omega_{s_n}})[k\Delta t], \tag{D1}$$

where N is the number of scales s_n used in the approximation and $\Delta s_n = s_n - s_{n-1}$. In practice these scales are chosen as a geometric series, i.e., $s_n = \ell e^{vn}$, where v is such that $s_N = T$.

In order to implement this sum, it is helpful to remark that, according to definitions (A2) and (A3), $\omega_{s_n}[k\Delta t]$ can be approximated as

$$\omega_{s_n}[k\Delta t] = \left(\theta_{s_N} \star \varepsilon_{s_N^{-1}\Delta t}\right)[k] + \sum_{m=n}^{N} \left(\theta_{s_m} \star \varepsilon_{s_m^{-2}\Delta t \Delta s_m}\right)[k\Delta t],$$

and therefore Eq. (D1) can be implemented as described in Algorithm 1.

Algorithm 1. Generate a sample of $X_\ell[k\Delta t]$.

$s \leftarrow s_N$
$\Delta s \leftarrow s_N - s_{N-1}$
Generate $\varepsilon_{s^{-1}\Delta t}[k]$
$\omega[k] \leftarrow (\theta_s \star \varepsilon_{s^{-1}\lambda^2\Delta t})[k]$
$X[k] \leftarrow \Delta s\, s^{H-2}\, (\psi_s \star e^{\omega})[k]$
$n \leftarrow N - 1$
while $[n > 1]$ **do**
  $s \leftarrow s_n$
  $\Delta s \leftarrow s_n - s_{n-1}$
  Generate $\varepsilon_{s^{-2}\Delta t \Delta s}[k]$
  $\omega[k] \leftarrow \omega[k] + (\theta_s \star \varepsilon_{s^{-2}\Delta t \Delta s})[k]$
  $X[k] \leftarrow X[k] + \Delta s\, s^{H-2}\, (\psi_s \star e^{\omega})[k]$
  $n \leftarrow n - 1$
return X

APPENDIX E: THE DISSIPATIVE ANOMALY

The dissipative anomaly is a property one expects in fully developed turbulence to conciliate the fact that, when the Reynolds number becomes arbitrarily large (i.e., the kinematic viscosity ν goes to zero), on one hand the gradient of the velocity field diverges (i.e., v becomes nondifferentiable since it corresponds to a global regularity close to $H = 1/3$) while the dissipation rate $\varepsilon \sim \nu(\frac{\partial v}{\partial x})^2$ remains finite. If one denotes by η the Kolmogorov scale, i.e., the scale above which v is smooth, from the behavior of the velocity increments, $(\delta_\ell v)^3 \sim \varepsilon \ell$, one can approximate the gradient as $\frac{\partial v}{\partial x} \sim \varepsilon^{1/3}\eta^{-2/3}$ so that the previous finite dissipation rate condition holds provided

$$\eta \sim \left(\frac{\nu^3}{\varepsilon}\right)^{1/4} \Leftrightarrow \nu \sim \varepsilon^{1/3}\eta^{4/3}. \tag{E1}$$

Let us see in what respect such a dissipative anomaly can hold within our model. For that purpose one has to seek a "viscosity" $\nu(\ell)$ such that, when $\ell \to 0$, $\nu(\ell) \to 0$ and there exists $0 < \varepsilon < \infty$ verifying

$$\lim_{\ell \to 0} \nu(\ell)\, \mathbb{E}\left[\left(\frac{\partial X_\ell(t)}{\partial t}\right)^2\right] = \varepsilon. \tag{E2}$$

Let us denote $\varphi'(t)$, the derivative of φ by $\vartheta(t)$. We thus have

$$\left(\frac{\partial X_\ell(t)}{\partial t}\right)^2 = \int_\ell^T \int_\ell^T (s_1 s_2)^{H-3} ds_1 ds_2 \iint e^{\omega_{s_1}(b_1)+\omega_{s_2}(b_2)} \vartheta \times \left(\frac{b_1 - t}{s_1}\right)\vartheta\left(\frac{b_2 - t}{s_2}\right) db_1 db_2.$$

Since ϑ is bounded and for $s_1 > s_2$ and

$$\mathbb{E}[e^{\omega_{s_1}(b_1)+\omega_{s_2}(b_2)}] \leqslant s_1^{-\phi(2)},$$

it results that

$$\nu(\ell)\, \mathbb{E}\left[\left(\frac{\partial X_\ell(t)}{\partial t}\right)^2\right] \leqslant K\nu(\ell) \int_\ell^T ds_2 s_2^{H-2} \int_{s_2}^T s_1^{H-2-\phi(2)},$$

which means that

$$\nu(\ell)\,\mathbb{E}\left[\left(\frac{\partial X_\ell(t)}{\partial t}\right)^2\right] = O\big(\nu(\ell)\ell^{2H-2-\phi(2)}\big).$$

In order to reproduce the dissipative anomaly it thus suffices to choose

$$\nu(\ell) \sim \ell^{2(1-H)+\phi(2)}. \tag{E3}$$

Let us see which kind of scaling Eq. (E3) leads to if one wants to fit turbulence within our framework. One can choose a normal law of $\omega_\ell(t)$ with intermittency coefficient $\lambda^2 = 0.025$ [63–65], i.e., $\phi(q) = q(q-1)\lambda^2/2$ satisfying $\phi(1) = 0$. The linear behavior of the third-order structure function leads to the choice $\zeta_3 = 1 = 3H - \phi(3) = 3H - 3\lambda^2$ and therefore $H = 1/3 + \lambda^2$. It thus results that Eq. (E3) can be rewritten as $\nu(\ell) \sim \ell^{2-2/3-2\lambda^2+\lambda^2} \sim \ell^{4/3-\lambda^2}$, which corresponds, up to the intermittency correction $-\lambda^2$, to the relationship (E1) obtained within the Kolmogorov approach to turbulence.

APPENDIX F: COMPUTATION OF THE LEVERAGE FUNCTION

The explicit expression of the leverage function (44) in the case of continuous wavelet cascade as defined in Eq. (9) is quite intricate:

$$\mathcal{L}_q(\tau) = Z_{q,\ell}^{-1}\int_0^T s^{H-2}ds \int \times\left[\varphi\left(\frac{-b}{s}\right) - \varphi\left(\frac{-b-\ell}{s}\right)\right]\mathbb{E} \times [e^{\omega_s(b)}|\delta_\ell X(\tau)|^q]db,$$

where $\delta_\ell X(t)$ stands for $X(t) - X(t-\ell)$. In order to study the behavior of such an expression, we will first make the following approximation:

$$\mathbb{E}[e^{\omega_s(t_1)}|\delta_\ell X(t_2)|^q] \simeq \ell^H \mathbb{E}[e^{\omega_s(t_1)+q\omega_\ell(t_2)}].$$

This approximation is hard to establish on rigorous grounds but can be intuitively motivated by the fact that when factorizing $\omega_\ell(t)$ in all $\omega_s(b)$ involved in $\delta_\ell X(t)$, the modulus of the remaining integral has almost vanishing correlations with $\omega_\ell(t')$ and $\delta_\ell X(t')$ for $|t'-t| > \ell$. We have checked numerically that when we effectively replace $|\delta_\ell X(t)|^q$ with $\ell^{qH}e^{q\omega_\ell(t)}$, the estimations of the leverage functions are basically unchanged. We are thus left to estimate the following integral (the factor ℓ^{qH} has been absorbed in the redefinition of $Z_{q,\ell}$):

$$\mathcal{L}_q(\tau) = Z_{q,\ell}^{-1}\int_0^T s^{H-2}ds\int db\,\mathbb{E}[e^{\omega_s(b)+q\omega_\ell(\tau)}]\delta_{\frac{\ell}{s}}\varphi\left(\frac{-b}{s}\right). \tag{F1}$$

Hereafter we will exclusively elaborate on the case $q = 1$ but the case of arbitrary q can be considered along the same lines. Let $C_{s,\ell}(z) = \mathbb{E}[e^{\omega_s(b)+\omega_\ell(b+z)}]$. Thanks to Eqs. (A5) and (A4) and given the condition $\phi(1) = 0$, we have $C_{s,\ell}(z) = C_{\max(\ell,s)}(z)$ with

$$C_{s'}(z) = \begin{cases} T^\gamma e^\gamma s'^{-\gamma} e^{-\gamma\frac{|z|}{s'}}, & \text{if } |z| \leqslant s', \\ T^\gamma |z|^{-\gamma}, & \text{if } T \geqslant |z| \geqslant s', \\ 1, & \text{if } |z| > T, \end{cases} \tag{F2}$$

where we have set $\gamma = \phi(2)$. For the sake of simplicity and without loss of any generality we set $T = 1$ in the following. We will also consider a simpler version of $C_s(z)$ (notably used, e.g., in Refs. [14,17]) that is easier to handle in numerical and analytical computations:

$$C_{s'}(z) = (s' + |z|)^{-\gamma}. \tag{F3}$$

Equation (F1) can then be rewritten as

$$\mathcal{L}_1(\tau) = Z_{1,\ell}^{-1}\int_0^1 s^{H-1}ds\int du\varphi(u)[C_{\max(s,\ell)}(\tau+su) - C_{\max(s,\ell)}(\tau+\ell+su)].$$

Let us decompose $\mathcal{L}_1(\tau)$ as $\mathcal{L}_1(\tau) = \mathcal{L}_-(\tau) + \mathcal{L}_+(\tau)$, where

$$\mathcal{L}_-(\tau) = Z_{1,\ell}^{-1}\int_0^\ell s^{H-1}ds\int du\varphi(u)[C_\ell(\tau+su) - C_\ell(\tau+\ell+su)],$$

$$\mathcal{L}_+(\tau) = Z_{1,\ell}^{-1}\int_\ell^1 s^{H-1}ds\int du\varphi(u)[C_s(\tau+su) - C_s(\tau+\ell+su)].$$

Let us choose $Z_{1\ell} = Z_1\ell$. In the range $s < \ell$, we can write (because φ is supported in $[-1, 1]$)

$$C_\ell(\tau+su) - C_\ell(\tau+\ell+su) \simeq -suC'_\ell(\tau+\ell).$$

Since, for $\tau > \ell$, $|C'_\ell(z)| = O(|\tau|^{-1-\gamma})$, the contribution of $s \in [0, \ell]$ in $\mathcal{L}_1(\tau)$ is therefore of order

$$\mathcal{L}_-(\tau) \sim Z_1^{-1}\ell^{-1}\tau^{-\gamma-1}\int_0^\ell s^H \sim Z_1^{-1}\ell^H\tau^{-1-\gamma}.$$

When $\ell < s$, we write

$$\mathcal{L}_+(\tau)\ 0 \simeq -Z_1^{-1}\int_\ell^1 s^{H-1}ds\int du\varphi(u)C'_s(\tau+su)$$

$$= -|\tau|^{H-1-\gamma}Z_1^{-1}\int_{\ell|\tau|^{-1}}^{|\tau|^{-1}} s^{H-1}ds \times\int du\varphi(u)C'_s(su\pm 1),$$

where the last expression results from the change of variable $s \to |\tau|^{-1}s$ and $\pm$ corresponds to the sign of the lag τ. Let us define (if both integrals converge)

$$C_+ = -Z_1^{-1}\int_0^{+\infty} s^{H-1}ds\int du\varphi(u)C'_s(su+1),$$

$$C_- = -Z_1^{-1}\int_0^{+\infty} s^{H-1}ds\int du\varphi(u)C'_s(su-1).$$

In the domain $\tau \gg \ell$, we thus have shown that

$$\mathcal{L}_1(\tau) \simeq C_\pm|\tau|^{H-1-\gamma}, \tag{F4}$$

where the constants C_+ and C_- correspond to the ranges $\tau > 0$ and $\tau < 0$, respectively. The amplitude of the "leverage effect" can thus be measured by the ratio

$$\kappa = \frac{C_+}{C_-}, \tag{F5}$$

which may strongly depend on the chosen wavelet φ.

[1] A. Kolmogorov, J. Fluid Mech. **13**, 82 (1962).
[2] A. Obukhov, J. Fluid Mech. **13**, 77 (1962).
[3] E. A. Novikov and R. Stewart, Isv. Akad. Nauk SSSR, Seria Geofiz. **3**, 408 (1964).
[4] B. B. Mandelbrot, J. Fluid Mech. **62**, 331 (1974).
[5] B. B. Mandelbrot, C. R. Acad. Sci. Paris **278**, 289 (1974).
[6] U. Frisch, *Turbulence* (Cambridge University Press, Cambridge, 1995).
[7] J. P. Kahane and J. Peyrière, Adv. Math. **22**, 131 (1976).
[8] Y. Guivarc'h, C. R. Acad. Sci. Paris **305**, 139 (1987).
[9] J. Barral, in *Fractal Geometry and Applications, Part 2, Multifractals, Probability and Statistical Mechanics, Applications*, Vol. 72 of Proceedings of Symposia in Pure Mathematics (American Mathematical Society, Providence, 2004), pp. 53–90.
[10] J. Barral and B. B. Mandelbrot, Prob. Theory Relat. Fields **124**, 409 (2002).
[11] J. F. Muzy and E. Bacry, Phys. Rev. E **66**, 056121 (2002).
[12] E. Bacry and J. F. Muzy, Commun. Math. Phys. **236**, 449 (2003).
[13] A. Arneodo, E. Bacry, S. Manneville, and J. F. Muzy, Phys. Rev. Lett. **80**, 708 (1998).
[14] J. F. Muzy, J. Delour, and E. Bacry, Eur. J. Phys. B **17**, 537 (2000).
[15] F. Schmitt and D. Marsan, Eur. Phys. J. B **20**, 3 (2001).
[16] B. B. Mandelbrot, A. Fisher, and L. Calvet, *A Multifractal Model of Asset Returns*, Cowles Foundation Discussion Paper, No. 1164 (Cowles Foundation for Research in Economics at Yale University, 1997).
[17] E. Bacry, J. Delour, and J. F. Muzy, Phys. Rev. E **64**, 026103 (2001).
[18] C. Ludena, Ann. Appl. Probab. **18**, 1138 (2008).
[19] L. C. P. Abry, P. Chainais, and V. Pipiras, IEEE Trans. Inf. Theory **55**, 3825 (2009).
[20] R. Benzi, L. Biferale, E. Calzavarini, D. Lohse, and F. Toschi, Phys. Rev. E **80**, 066318 (2009).
[21] B. Pochart and J. P. Bouchaud, Quantitative Finance **2**, 303 (2002).
[22] E. Bacry, L. Duvernet, and J. F. Muzy, J. Appl. Probab. **49**, 482 (2012).
[23] L. Chevillard, C. Garban, R. Rhodes, and V. Vargas, arXiv:1712.00332.
[24] L. F. Richardson, *Weather Prediction by Numerical Process* (Cambridge University Press, Cambridge, UK, 1922).
[25] S. Mallat, *A Wavelet Tour of Signal Processing* (Academic Press, San Diego, 1999).
[26] A. Arneodo, E. Bacry, and J. F. Muzy, J. Math. Phys. **39**, 4124 (1998).
[27] J. Barral and S. Seuret, C. R. Acad. Sci. Paris Ser. I **341**, 353 (2005).
[28] A. Arneodo, E. Bacry, S. Jaffard, and J. F. Muzy, J. Stat. Phys. **87**, 179 (1997).
[29] A. Arneodo, E. Bacry, J. F. Muzy, and S. Jaffard, J. Fourier Anal. App. **4**, 159 (1998).
[30] F. Schmitt and D. Marsan, Eur. Phys. J. B **20**, 3 (2001).
[31] A. Arneodo, C. Baudet, F. Belin, R. Benzi, B. Castaing, B. Chabaud, R. Chavarria, S. Ciliberto, R. Camussi, F. Chilla *et al.*, Europhys. Lett. **34**, 411 (1996).
[32] W. Feller, *An Introduction to Probability Theory and Its Applications*, Vol. II (John Wiley & Sons, Inc., 1971), 2nd ed.
[33] B. B. Mandelbrot, Sci. Am. **280**, 70 (1999).
[34] Z. S. She and E. Lévêque, Phys. Rev. Lett. **72**, 336 (1994).
[35] This effect, first discussed in the pioneering work of Molchan [66,67] and considered more recently, e.g., in Ref. [68], mainly corresponds to a nonergodic behavior in the scaling exponents of high-order structure functions.
[36] J. Delour, Ph.D. thesis, Université de Bordeaux I, Pessac, France, 2001.
[37] M. Taqqu and G. Samorodnisky, *Stable Non-Gaussian Random Processes* (Chapman & Hall, New York, 1994).
[38] J. F. Muzy, E. Bacry, and A. Arneodo, Phys. Rev. E **47**, 875 (1993).
[39] M. Holschneider and P. Tchamitchian, Invent. Math. **105**, 157 (1991).
[40] J. F. Muzy, E. Bacry, and A. Arneodo, Phys. Rev. Lett. **67**, 3515 (1991).
[41] G. Parisi and U. Frisch, in *Proceedings of the International School on Turbulence and Predictability in Geophysical Fluid Dynamics and Climate Dynamics*, edited by M. Ghil, R. Benzi, and G. Parisi (North-Holland, Amsterdam, 1985), p. 84.
[42] S. Jaffard, SIAM J. Math. Anal. **28**, 944 (1997).
[43] S. Jaffard, SIAM J. Math. Anal. **28**, 971 (1997).
[44] J. Barral and B. B. Mandelbrot, in *Fractal Geometry and Applications, Part 2, Multifractals, Probability and Statistical Mechanics, Applications*, Vol. 72 of Proceedings of Symposia in Pure Mathematics (American Mathematical Society, Providence, 2004), pp. 3–52.
[45] M. Rambaldi, E. Bacry, and J. F. Muzy, arXiv:1807.07036.
[46] B. Mandelbrot and J. W. V. Ness, SIAM Rev. **10**, 422 (1968).
[47] B. Castaing, B. Chabaud, F. Chillà, B. Hébral, A. Naert, and J. Peinke, J. Phys. III **4**, 671 (1994).
[48] B. Castaing, Y. Gagne, and E. Hopfinger, Phys. D (Amsterdam, Neth.) **46**, 177 (1990).
[49] G. L. Eyink and K. R. Sreenivasan, Rev. Mod. Phys. **78**, 87 (2006).
[50] C. Meneveau and K. R. Sreenivasan, J. Fluid Mech. **224**, 429 (1991).
[51] Y. Pomeau, J. Phys. France **43**, 859 (1982).
[52] J.-P. Bouchaud, A. Matacz, and M. Potters, Phys. Rev. Lett. **87**, 228701 (2001).
[53] J. Perello and J. Masoliver, Phys. Rev. E **67**, 037102 (2003).
[54] B. Pochart, Ph.D. thesis, Ecole Polytechnique, Palaiseau, France, 2003.
[55] L. Chevillard, R. Robert, and V. Vargas, Europhys. Lett. **89**, 54002 (2010).
[56] R. M. Pereira, C. Garban, and L. Chevillard, J. Fluid Mech. **794**, 369 (2016).
[57] C. W. Misner, K. S. Thorne, and J. A. Wheeler, *Gravitation*, Physics Series (W. H. Freeman, San Francisco, 1973), 1st ed.
[58] J. F. Muzy and R. Baïle, Phys. Rev. E **93**, 052305 (2016).
[59] J. Kahane, Ann. Sci. Math. Québec **9**, 105 (1985).
[60] R. Rhodes and V. Vargas, Probab. Surveys **11**, 315 (2014).
[61] P. Billingsley, *Convergence of Probability Measures* (John Wiley & Sons, Inc., 1968).

[62] J. Swanson, Probab. Theory Relat. Fields **138**, 269 (2007).
[63] A. Arneodo, J. F. Muzy, and S. Roux, J. Phys. II France **7**, 363 (1997).
[64] A. Arneodo, S. Manneville, and J. F. Muzy, Eur. Phys. J. B **1**, 129 (1998).
[65] O. Chanal, B. Chabaud, B. Castaing, and B. Hebral, Eur. Phys. J. B **17**, 309 (2000).
[66] G. M. Molchan, Commun. Math. Phys. **179**, 681 (1996).
[67] G. M. Molchan, Phys. Fluids **9**, 2387 (1997).
[68] J. F. Muzy, E. Bacry, R. Baïle, and P. Poggi, Europhys. Lett. **82**, 60007 (2008).